New Phenomena of Anodic and Cathodic Crystal Growth.

By

Anilprasanna Goswami, M.Sc.

A Thesis Submitted for the
Degree of Doctor of Philosophy
in the University of London.

Applied Physical Chemistry Laboratories,
Imperial College, London, S.W.7.

June, 1950.

Contents.

Abstract of Thesis

entitled

New Phenomena of Anodic and Cathodic Crystal Growth.

by A.Goswami.

Crystal growth in anodic and cathodic processes was studied by electron diffraction. A similar study was also carried out on the oxidation of metals by other processes and chemical replacement of metals for comparison purposes. (110) and (100) faces of copper single crystals were mainly used in this experimental work. In some cases single crystals of iron were also used and in others polycrystalline copper, brass and iron.

The results showed that epitaxial growth of Cu_2O and CuO occurred in the initial stage of the anodic oxidation of copper single-crystal surfaces; with increasing oxide deposit thickness, however, the crystal arrangement of the CuO degenerated into a one degree orientation. Oxidation of a copper single crystal by immersion in water or in an alkaline solution produced mainly crystalline cuprous oxide in two degree orientation, though in some cases faint traces of CuO were also obtained. There was always parallel orientation of Cu_2O on Cu $\{110\}$ crystal faces. Twinning of Cu_2O on Cu (111) was observed and apparently initiated stable epitaxial

orientations with (114) and (221) planes of Cu_2O parallel to (110) and (100) planes of the copper substrate.

A phenomenon new in the solid-liquid type of reaction was observed in the case of epitaxially orientated Cu_2O formed on Cu by immersion in caustic soda solution. This consisted of the relief of epitaxial strain between the Cu_2O-Cu (110) interface by a process of "Rotational slip" about [110].

Another new phenomenon observed was the transformation of one degree orientated CuO to two degree orientated CuO by light unidirectional rubbing with cotton wool. This was explained in terms of the probable lath shape of the fragments broken off by cleavage during its rubbing.

In anodic treatment of Cu in acid solution, a strong inner potential refractive effect was noted and from the measurement of the displaced spots the inner potential of Cu was calculated for the (111) face. A strong disorientating effect on the substrate surface region was also observed in the anodic etching process at high current density.

In the formation of Cu_2Cl_2 and Cu_2Br_2 by anodic or halogen vapour reactions on Cu (110) a (111) orientation was observed and twinning of Cu_2Br_2 on (111) plane was also noted.

Epitaxial growth of Cd, Zn and Fe on Cu (110) and Cu (100) was studied. The orientations found on Cu (110) were (103) for Cd, (205) for Zn and (211) for Fe. A 15% compression

of the c axis was observed in the case of Zn epitaxially grown on Cu (110). Another interesting case of relief of epitaxial strain by "Rotational slip" was found in the case of (103) orientation of Cd on Cu (110).

The effects of superposition of alternating current on direct current in cathodic crystal growth were also investigated.

The influence of magnetic fields on crystal growth and orientation in cathodic deposits was studied in the case of iron. It was found that the magnetic field caused no change in orientation, but the crystals had a tendency to grow along the direction of the lines of force. An attempt has been made to correlate the crystal habit of iron electrodeposited in a magnetic field with the corresponding Bitter figures.

The phenomenon of chemical displacement was investigated The lattice constants of Cu (and of the Cu_2O obtained from Cu) and Ag, obtained by displacement were measured and a mechanism of the process is suggested.

General Introduction.

In an ideal crystal the atoms or ions occupy the minimum potential energy configuration. Due to the actions of interatomic forces the atoms or ions are clustered together to pack themselves closely and form a three dimensional pattern. The crystal grows atom by atom, layer by layer, though growth of succeeding layers may, and indeed generally does, start before a layer is completed. Each atom, as it deposits on the surface of the crystal, takes up a position compatible, in terms of potential energy, with the surrounding conditions. The site of the deposited atoms or ions are then principally determined by the positions of the atoms or ions in the initial surface and subsequently by those of the atoms or ions in the new surface of the crystal. When the new growing surface has attained a thickness of the order of three or four atom layers, further growth is, in general, no longer directly influenced by the substrate; though interfacial strain effects between substrate and deposit may lead to disturbances such as twinning and rotational slip.

Crystals can be grown from the vapour, solution or melt of a substance or by a chemical reaction between the gas, liquid or solid, or by discharge of ions as in the electro-deposition process. The experimental work that will be

presented in the following chapters is mainly concerned with anodic and cathodic crystal growth. The advantages peculiar to this mode of crystal growth in studying epitaxial relationships will be outlined later.

The structures of electrodeposited coatings have been studied by many workers, e.g. Wood (1931) by X-rays, Thomson (1931), Cochrane (1936) and, in particular, Finch and his collaborators (1936, 1937 and 1947) by electron diffraction. Finch and his collaborators have shown that there are three distinct stages in the crystal growth of electrodeposits. In the initial stage of crystal growth, the orientation of the deposit is greatly influenced by the substrate structure, tending to cause orientated overgrowth (epitaxial growth, see below). The second is a transition stage in which the deposit crystals tend to become randomly disorientated. In the final stage, the orientation and the habit of the deposit crystal are determined by the bath conditions, i.e. temperature, current density, adsorption of ions or atoms at the cathode, etc.

When the temperature of the solution is high, the crystals tend to grow laterally, due to the high mobility of atoms or ions, the densest atomic plane growing parallel to the surface. At lower temperatures, the lateral growth is not favoured and due to the rapid exhaustion of ion concentration near the cathode the ions tend to be deposited on the projecting

parts of the surface so that outgrowths develop mainly along the normal to the surface and a densely populated plane tends to develop along the normal to the surface along which the densest atom row generally lies.

Many workers have observed parallel growth of the deposited crystal on a substrate. Royer (1928) after an extensive study of crystal growth on various substrates and considerations of crystal structures which had been determined by X-ray diffraction methods concluded that the deposited atoms or ions take such an orientation as to follow the substrate surface structure as far as possible, that is with a close fit between the two-dimensional arrangements of the deposited and the substrate atoms at the interface. He found that in such cases there was at least one densely populated lattice row in the deposit parallel to one in the substrate provided their relative identity spacings did not differ by more than 15%. This phenomenon was termed 'epitaxy'. Rudiger (1937) after studying the evaporated metals on single crystal substrates like calcite, mica, etc. found that a substrate must be heated to a certain temperature before the growth proceeds epitaxially. Finch and Whitmore (1938) have shown that short (in the atomic sense) range forces act during the epitaxial crystal growth. Elleman and Wilman (1948) have suggested that during the epitaxial growth, both the

atomic fittings and the lattice fittings are of importance. Thomson and Cochrane (1939) and Thomson (1948) suggested that steps or cracks on a crystal surface might play an important part in the crystal orientation. According to them, atoms or ions will tend to form rows aligned along the crack and such a row then becomes the zone axis of the deposit crystals and hence governs the common orientation. Such a topographical feature is unlikely to determine the deposit orientation, though it may affect the localisation of the crystal nuclei first formed. Drabble (1949), working in this laboratory, has shown that on a diamond-ruled glass surface methylene blue crystals do not grow in any definite orientation, but develop their characteristic needle-shaped habit especially strongly when the needle axis is along a scratch. The clearest possible demonstration that steps or cracks do not determine epitaxial orientation is obtained both from the observation of well defined angles of rotational slip of atomic sheets over each other and from the adherence of the orientated pre-existing crystals (Wilman, 1950).

In the light of the above discussion it seems it will be useful to observe and examine new cases of epitaxial growth, in anodic and cathodic processes, in order to see more clearly the nature of the forces or factors that determine epitaxy. Unless the deposit is the same as the substrate, there will not

be an exact 'fit' in the lattice position between the substrate and the deposit interface, and such misfit must give rise to strain in the deposit at some distance above the substrate-deposit interface. The effects of such a strain on the deposit crystals have not yet been fully elucidated in the case of electrodeposits, though it is known that twinning in the deposit is most likely due to such strain. Evans and Wilman (1950) have shown that epitaxial strain in chemically formed deposits may result in rotational slip in the deposit crystals. These considerations are of great importance to an understanding of the distribution and magnitude of the surface forces of the substrate, particularly in relation to the adhesion between the deposit and substrate, and the general properties of the cathodic and anodic deposits.

The structures of metallic cathodic deposits have been investigated by Blum and Rawdon (1923), Graham et al (1923) and Hothersall (1935) by optical microscopy; by Wood (1931), Hume-Rothery and Wyllie (1943) and others with X-rays; and by Thomson (1931), Cochrane (1936) and Finch and his collaborators (1936, 1937, 1947) by electron diffraction. Finch, Wilman and Yang (1947) have shown the importance of adsorbed hydrogen atoms or ions at the cathode in modifying the orientation of the crystals in a thick deposit. A superposed alternating current on direct current might well affect the adsorption of hydrogen

ions and atoms at the cathode, and if so could be expected to cause a change in the orientation of the thick deposits. Such a study should also throw light on the nature of hydrogen adsorption at the cathode.

Comparatively little work has been carried out on anodic crystal growth. In this laboratory Sun (1934) and Lamchen (1937) have examined by electron diffraction anodic oxidation products formed on polycrystalline substrates, and recently Feitknecht and Lenel (1948) and Huber and Bieri (1948) have studied by electron microscopy and X-rays. The most interesting conclusion to be drawn from this latter work is that electron diffraction affords by far the most powerful method of attack in this field. A further study by electron diffraction of the crystal growth on single crystals in anodic oxidation will be useful in showing the mode of the crystal growth in the initial as well as in the subsequent stages.

The present work falls into three sections.

a. The first deals with the study of the anodic oxidation processes, with special reference to crystal growth in the initial stage and the variation of orientation with change in conditions. Comparative experiments have also been carried out, in that the oxidation has been effected by other methods such as oxidation in solution or in gases.

b. The second section deals with the epitaxial crystal

growth of different metals, the effect thereon of alternating currents superimposed on the direct current in the cathodic crystal growth, and the influence of a magnetic field on cathodic crystal growth.

c. The final section deals with the phenomena of chemical displacement with special reference to the lattice constant measurement and epitaxial crystalline growth.

As substrate surfaces, single crystals of copper (110) and (100) faces and iron (100) were for the most part used. This greatly facilitated interpretation. Any change in the structure of the deposits or their orientation with respect to the substrate could be easily followed step by step by examining the surface. Again any disorientation caused during the crystal growth process could be observed with precision.

In some cases polycrystalline iron, copper and brass were used, where the initial stage of crystal deposit was of secondary importance.

In all these investigations the electron diffraction method was used for examining the surface structure. The penetrating power of about 60 KV. electrons is very low, being confined to about 10-20 atoms depth below an atomically smooth surface when the beam grazing incidence angle was of the order of 30'. Further, the scattering of electrons by the atoms is so efficient that the patterns are visible on a fluorescent

screen and can be recorded photographically with only a short exposure time.

The electron diffraction camera used was of the standard Finch type. The principle and applications of electron diffraction have already been discussed by Finch and Wilman (1937) and hence are not included here.

SECTION I.

Crystal Growth in Anodic Oxidation Processes and a Comparison with Other Oxidation Processes.

Introduction.

Anodic oxidation has been studied by various workers. Due to its special applications for imparting corrosion resistance properties to various metals such as Cu, Fe, and certain ferrous alloys, Al, Mg and their alloys, a study of this subject has attained a special significance in recent years.

Müller (1931) and Hedges (1932), after studying the process, particularly in relation to passivity of the metal, found that at the anode, one of the following may happen.

a) The metal goes into solution; (b) the metal goes into solution at a lower current density, but becomes passive at a higher current density; (c) an insoluble adherent compound is formed; or (d) the metal becomes passive and thus no longer reactive.

Schiemedt (1908) obtained what he believed to be cupric oxide by anodic treatment of copper. Bengough and Stuart (1923) patented a process to obtain oxide of aluminium by anodic treatment in 3·0% chromic acid solution. Anodic oxide coatings on aluminium and its alloys have also been

obtained by treating in various other electrolytes such as H_2SO_4, H_3BO_3 etc. (Jenny, 1940).

Sun (1934) and Lamchen (1937) in this laboratory have studied by electron diffraction the anodic crystal growth process. They observed that most of the metals give rise to crystalline compounds, mostly oxides, which often have preferred orientations, with a densely packed net plane parallel to the substrate surface. Ni forms NiO with (110) faces parallel to the substrate, but the crystals are otherwise unorientated. Lamchen (1937) examined also the anodic oxide coatings formed on aluminium and found that the coating was amorphous and thus similar in nature to the air-formed oxide. Harrington and Nelson (1940) found that by anodic treatment of Al in H_2SO_4 or H_3BO_3 or other electrolytes, the oxide formed was amorphous but on prolonged boiling in water was converted into boehmite ($Al_2O_3.H_2O$) which, on igniting in air, was converted to γ-Al_2O_3. They also found that on Ta and Ti, the coatings formed are sometimes crystalline and sometimes amorphous. They reported that when the anodic oxide coating on Al was heated to about 650°C., no change in structure occurred. More recent work in this laboratory (de Brouckere) showed that prolonged heating resulted in γ-Al_2O_3 being formed.

Halliwell (1948), working in this laboratory, showed that the amorphous film on anodised aluminium was converted into

crystalline γ-form by igniting in air for a minute only. Usmani (1941) obtained two-degree orientated Cu_2Br_2, Cu_2I_2 by treating a (111) face of Cu anodically in bromide or iodide solution. Huber and Bieri (1948) studied the oxidation of a cleavage face of a Zn single crystal in N/10 NaOH solution at room temperature. They observed ~~that~~ (0001) orientation of the ZnO coating ~~was obtained.~~

Feitknecht and Lenel (1944) examined the anodic oxide coating on polycrystalline Cu by electron microscopy and X rays and concluded that at first Cu_2O was formed, which was later converted into CuO (tenorite), and that in an unstirred ~~oxidising liquid~~ soln a film of $Cu(OH)_2$ is formed over the surface. The evidence is rather indirect; from electron microscope photographs it is only possible to distinguish the formation of different compounds from their habit and this is sometimes ambiguous. The X ray data are also not available.

The formation of Cu_2O and its quick conversion to CuO by anodic oxidation in an alkaline bath at room temperature was also reported by Hickling and Taylor (1948) from a study of variation of potential by an oscillographic method. Here again the conclusion is rather an indirect one. Frisby (1949) examined the anodically treated single crystals as well as polycrystalline copper in N/10 NaOH by electron diffraction. He could not get any distinct clear pattern from the anodically treated surface, and could not therefore identify the compound formed.

Probably his technique was at fault. But he reported that on boiling in water the compound gave a sharper pattern which had no preferred orientation at all. He identified the compound formed, after boiling the anodically treated surface in water, as CuO.

From the above survey of anodic oxidation processes, it is seen that though the chemical nature of the compounds formed on oxidised metal surfaces are generally known, their crystal structures, the modes of growth, the crystalline orientations and habit are not yet fully explored. Moreover, how far this anodic crystal growth process is analogous to the cathodic crystal growth mechanism discussed by Finch and his coworkers (1947) is a matter of great interest. Further, an analogy of this process with the general process of oxidation might be drawn by a comparative study with the oxidation processes in solutions or in contact with dry air or oxygen. A brief survey of the work on oxidation of metals is given below.

Thomson (1931) obtained two degree orientated Cu_2O on Cu single crystals. Yamaguti (1938) studied the formation of single crystals of Cu_2O on Cu (100) and Cu (111) faces at about 1000°C. and observed that often cube axes of Cu_2O were parallel to cube axes of Cu, but that sometimes another orientation was also developed. Preston and Bircumshaw (1935) studied the

formation of Cu_2O on polycrystalline copper. Thomson (1931) obtained, by electron diffraction, a pattern due to an oxide of copper which he could not identify from structures of Cu_2O and CuO known at that time. Murison (1934) and Miyake (1936) obtained a compound, CuO' by heating copper in air. Tunnell and his co-workers (1935) determined the structure of CuO by X-rays and found it to be monoclinic and not triclinic as had hitherto been supposed. It was shown by Finch (1938) that the pattern obtained by Thomson was really a mixture of Cu_2O and CuO. Thus the oxide obtained by Miyake and Murison was also CuO. Leu (~~1950~~), working in this laboratory, has observed that electropolished Cu (111) forms an amorphous film both at room temperature and at 100°C., but on treatment in water it is converted into crystalline Cu_2O.

Oxidation of Fe at room and higher temperatures has been studied by Mehl and his co-workers (1934), Nelson (1937) and Miyake (1937).

The oxide film formed on Zn at room temperatures has been studied by Finch and Quarrell (1933-34) and they observed pseudomorphism of ZnO on Zn (001). On heating such ZnO regains its normal axial ratio. Acharya (1948) observed (001) ZnO on a cleavage plane of zinc.

Preston and Circumshaw (1936) were the first to show directly by electron diffraction, in transmission technique,

that the spontaneously formed oxide on aluminium was amorphous at room temperature and began to be converted into crystalline γ-Al_2O_3 on prolonged heating to about 700°C.

Wilman (1940) has obtained two degree orientated silver halides by the reaction of halogen vapours on silver film. Usmani (1941) as referred to before, obtained two degree orientated Cu_2Br_2 and Cu_2I_2 with (111) planes parallel to (111) surfaces of the Cu single crystals.

The growth of oxide films at room temperature and at high temperature has been discussed theoretically by Cabrera and Mott (1949). They believed that during the formation of oxide coatings, metal ions diffuse through the oxide layers to combine with oxygen adsorbed on the surface. Finch (1950) showed that in many cases oxygen actually diffuses through the crystal boundaries down to the metal.

2. Experimental.

a. Preparation of single crystal substrates.

The copper single crystals used in the present work were cut from a copper single crystal rod, about 1 cm. in diameter, which was kindly lent by Professor Finch for the present investigations. The single crystal was carefully cut with a jeweller's saw lubricated with watch oil, so as to avoid much distortion of the crystal. The cut pieces of

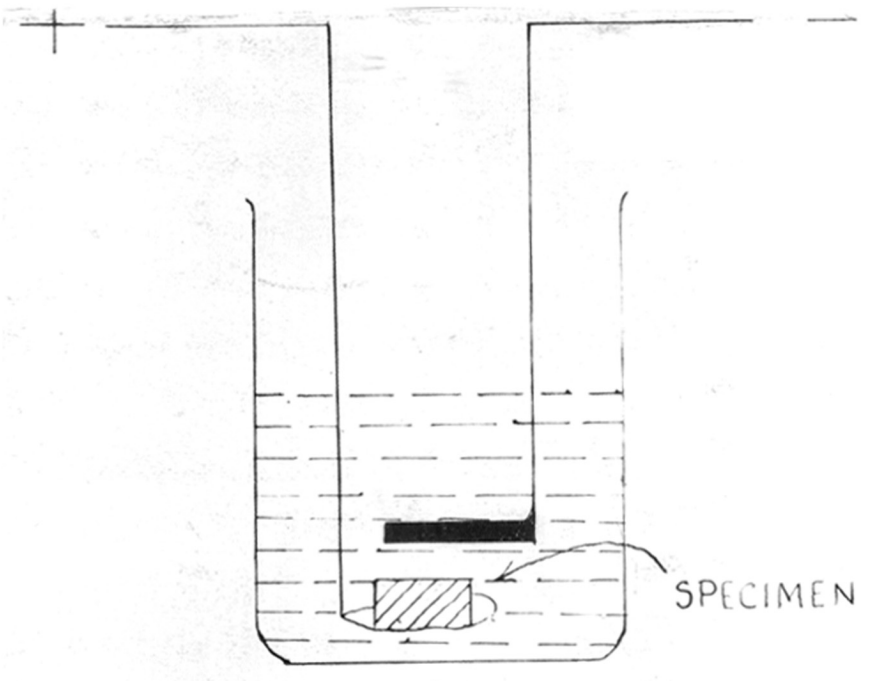

FIG. 1

crystals were then ground slowly with emery paper, of grades 1, 0, 00, 000 and 0000, successively, lubricated with benzene, so as to develop a face. The crystals were then etched in 1:1 HNO_3 to remove the distorted layers and then electropolished in a solution recommended by Jacquet (1936), containing 63% by weight of H_3PO_4 and 37% by weight water, at room temperature. The concentration of H_3PO_4 was not very critical for electropolishing. The current and voltage were controlled by a rheostat. The voltage was maintained between 2 and 3 volts, taking care that no gas evolution took place at the anode surface. The cathode was a sheet of copper bent at right angles and was kept about 3 cm. above the anode surface, as shown in Fig.1. The surfaces to be electropolished were kept horizontal below the cathode surface. After electropolishing the copper crystals were taken out, thoroughly washed with distilled water, then dipped into 5% KCN solution to remove any trace of oxide formed on the surface during electropolishing, and finally transferred, after appropriate washing (H_2O followed by alcohol), to the electron diffraction camera, under propyl alcohol. From the pattern the direction of the copper surface was identified, relative to the copper lattice. The crystals were then further ground and electropolished as before to prepare the desired faces and were again examined in the diffraction camera before any further experiments were

F 4849

Fig 2

Cu(110), beam along cube face diagonal

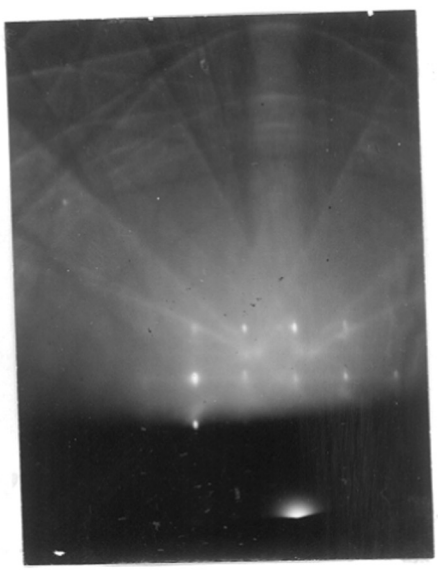

F 4852

Fig 3

Cu (100), beam along the cube edge

carried out on them.

Single crystals of Cu, (110) and (100) surfaces, treated in this way yielded the patterns shown in Fig.2 and Fig.3. The sharp elongated diffraction spots together with Kikuchi lines show the smoothness (atomically) of the surfaces and high lattice perfection of the crystals.

b. Anodic oxidation process.

The specimens to be used as anodes were surrounded by a hollow cylindrical copper cathode, about 6 cm. in diameter, immersed in the electrolyte. The temperature of the electrolyte was noted from the thermometer reading and was maintained within $\pm$ 2°C. The specimens were immersed first in the bath, allowed to attain the temperature of the bath approximately during one minute, and then the current was switched on for anodic oxidation. Afterwards the specimens were taken out of the bath, washed thoroughly in distilled water, and transferred to the diffraction camera under propyl alcohol. The current passed was measured with a milliammeter, and the current density was calculated from the known area of the anode specimens.

c. Other oxidation processes.

The freshly resurfaced copper crystals were also oxidised by immersion in alkali solution, or water, by heating in air or by exposing them to halogen vapours. Halides were also formed by immersion in a halide solution. Cu_2Cl_2 was

formed on the copper crystals by reaction with chlorine, which was prepared by dropping concentrated HCl into a strong solution of $KMnO_4$ and collecting the chlorine in a test-tube. The copper crystal was brought near the test tube and the vapour was allowed to react with the specimen in presence of air for a few seconds. It was then transferred quickly to the diffraction camera under propyl alcohol and examined in vacuo.

3. Results.

a. Anodic oxidation of a Cu (110) face in an alkaline solution.

When copper was oxidised anodically in NaOH solution a coating was formed which varied in colour from brownish to greenish to matt jet black, depending upon the temperature, concentration of the solution and the time of treatment. When the oxidation was carried on for about 10 minutes or more, evolution of oxygen took place at the anode. The electron diffraction patterns obtained by treating Cu (110) in 10% NaOH solution with 10 ma./sq.cm. for about 5 minutes at 80°C. were similar to Fig.4. The coating was matt jet black in appearance. The specimen was examined in two or more azimuths and in all cases the pattern remained the same, indicating that the coating was one-degree orientated with a net plane parallel to the Cu (110) substrate. From the measurement of

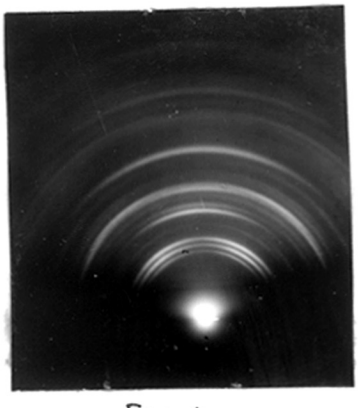

Fig 4

CuO at 10 mA/cm² at 80°C.

the ring radii the net-plane spacings were calculated as shown in Table I. They correspond well to the spacings of CuO obtained by Tunnell, Posnjak and Ksanda (1935) by X-ray diffraction on the powdered mineral tenorite.

Table I.

Intensity	Radius in cms.	d spacing in A.	Diffraction indices hkl	X-ray spacings (Tunnell and co-workers) in A.
s	0.930	2.742	110	2.737
s	1.021	2.497	$\bar{1}11$ 002	2.513
s	1.105	2.304	111 200	2.307
f	1.301	1.957	$\bar{1}12$	1.954
mf	1.375	1.854	$\bar{2}02$	1.855
vvf	1.450	1.755	112	1.769
s	1.493	1.705	020	1.705
m	1.577	1.615	021	1.615
f	1.609	1.582	202	1.575
f	1.697	1.497	$\bar{1}13$	1.499
s	1.805	1.411	022 310 $\bar{3}11$	1.411
S	1.860	1.369	220 113	1.370
vf	1.951	1.304	311 $\bar{3}12$ 221	1.298
vf	2.021	1.260	004 $\bar{2}22$	1.258
m	2.185	1.165	$\bar{3}13$ 222	1.163
s	2.337	1.087	$\bar{1}31$	1.086

s = strong; m = medium; f = faint; v = very.

The structure of copper (cupric) oxide, according to them, is monoclinic with the following parameters:

$a = 4.653$ A.

$b = 3.410$ A.

$c = 5.108$ A.

$\beta = 99° 29'$

with Cu atoms at $\frac{1}{4}\frac{1}{4}0$, $\frac{3}{4}\frac{1}{4}\frac{1}{2}$, $\frac{3}{4}\frac{3}{4}0$, $\frac{1}{4}\frac{3}{4}\frac{1}{2}$

and oxygen atoms at $0u\frac{1}{4}$, $0\bar{u}\frac{3}{4}$, $\frac{1}{2}(u+\frac{1}{2})\frac{1}{4}$, $\frac{1}{2}(\frac{1}{2}-u)\frac{3}{4}$

where $u = 0.\overline{58}$.

The strong 020 ring and the medium 021 ring in the plane of incidence apparently suggest that the orientation of the CuO is with either {010} or {021} parallel to the surface, ~~and~~ or both of them are present. As the structure of the CuO is monoclinic an extension of the usual method (Finch and Wilman, 1937) had to be used to decide the orientation by comparing the pattern with the theoretical one to be expected in different orientations.

The theoretical pattern has been calculated in the following way, developed in this laboratory by H.Wilman. For lattice row [uvw] to be normal to any plane (hkl) it must have

$$u : v : w = \underline{r}^*.\underline{a}^* : \underline{r}^*.\underline{b}^* : \underline{r}^*.\underline{c}^*$$

$$= 1/a \left\{ (h/a) \sin^2\alpha + (k/b)(\cos\alpha\cos\beta - \cos\gamma) + (l/c)(\cos\alpha\cos\gamma - \cos\beta) \right.$$

$$: 1/b \left\{ (h/a)(\cos\alpha\cos\beta - \cos\gamma) + (k/b)\sin^2\beta + (l/c)(\cos\beta\cos\gamma - \cos\alpha) \right\}$$

$$: 1/c \left\{ (h/a)(\cos\alpha\cos\gamma - \cos\beta) + (k/b)(\cos\beta\cos\gamma - \cos\alpha) + (l/c)\sin^2\gamma \right\}$$

For monoclinic crystals this becomes

$$u : v : w = 1/a \left\{ h/a - (l/c)\cos\beta \right\} : 1/b \left\{ k/b \sin^2\beta \right\} : 1/c \left\{ -(h/a)\cos\beta + l/c \right\}$$

For CuO

$$u : v : w = \left\{ h(.04619) + l(.00693) \right\} : \left\{ k(.08364) \right\} : \left\{ h(.00693) + l(.03833) \right\}$$

and for (021) orientation

$$u : v : w = 0.693 : 16.73 : 3.83.$$

The diffraction spots lie on layer lines of order h' given by $h' = hu + kv + lw$

$$\therefore \quad h'_{021} = 37.29$$

Assuming $\lambda L = 10$, then the radius for (021) = 6.19 cm., and hence one h' unit = 0.166 cm.

$$R = \frac{\lambda L}{d_{(021)}} = 6.19.$$

$$h'_{unit} = \frac{6.19}{37.29} = 0.166 \text{ cm}$$

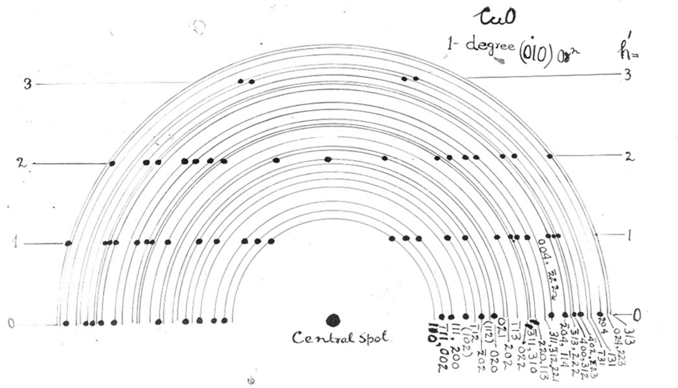

Fig 5

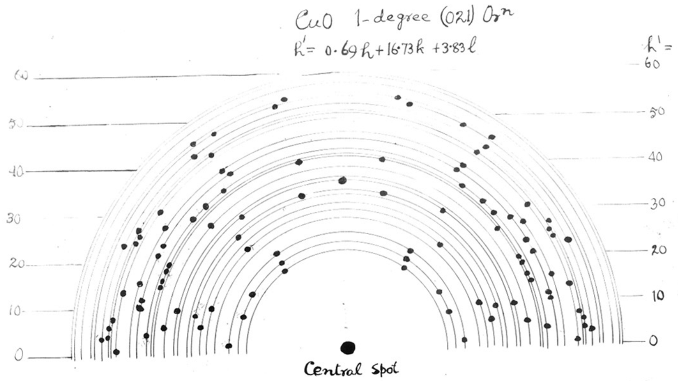

Fig 6

Theoretical patterns of CuO, with (010) and (021) orientations

Similarly for the (010) orientation layer line $h'_{010} = 1$. The theoretical patterns for (010) and (021) orientations are shown in Figs. 5 and 6. In the theoretical pattern of (010) orientation of CuO, it is seen that all the arcs lie on well-defined layer lines. The absence of such well-marked layer lines in the CuO pattern by anodic oxidation, Fig.4, coupled with the fact that the medium 021 arc is not in the same layer line as the 020 arc suggests that the orientation is not (010). This is more evident from the positions of the $\bar{1}12$, $\bar{2}02$, 112 arcs in the figure.

Comparing the positions of the arcs in the theoretical (021) orientation (Fig.6) with those in Fig.4, it is evident that there are similarities in the positions of the arcs, though the 020 arc should appear in a position slightly away from the plane of incidence (Fig.6), whereas in Fig.4, it is in the plane of incidence and of strong intensity. This can be accounted for by assuming that when rather long arcs appear near the plane of incidence they will coalesce and overlap so as to give high intensity there. Thus the orientation of CuO in Fig.4 appears to be (021).

(ii) Effects of Current Density.

The Cu (110) face was anodically oxidised at different current densities in 10% NaOH solution. The results are shown in Table 2.

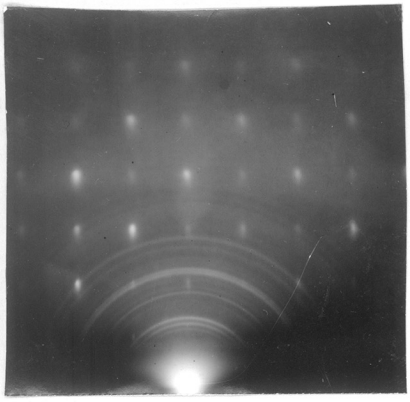

Fig 7
Cu_2O and CuO
c.d 5mA/cm²
Beam ⟨001⟩

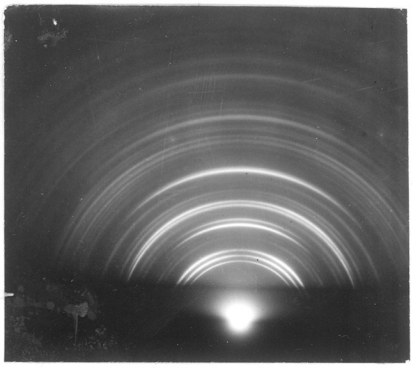

Fig 8
CuO
c.d. 10mA/cm²

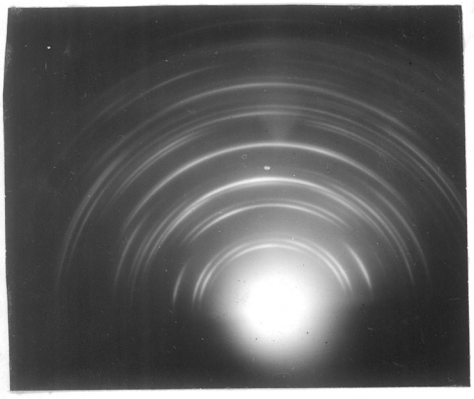

Fig 9
CuO
c.d. 22 mA/cm²
for 1½ min

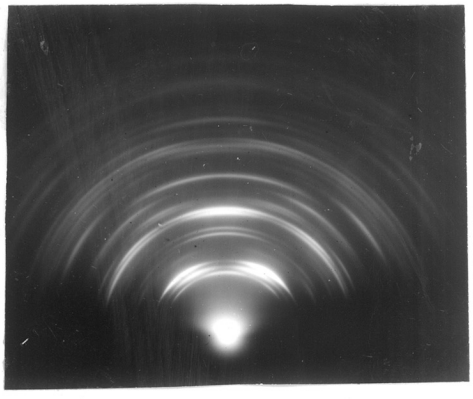

Fig 9a
CuO
c.d. 22mA/cm² for 4 mins.

Table 2.

Subst.	Current density ma/cm^2	Temp. °C.	Time mins	Orientation	Appearance	Fig.
Cu(110)	5	80	9	(110)Cu_2O // (110)Cu $[1\bar{1}0]Cu_2O$ // $[1\bar{1}0]Cu$ Random CuO	Brownish coating and at some places greyish appearance.	7
Cu(110)	10	80	5	(021)CuO // (110)Cu One degree orientated CuO	Black coating	8
Cu(110)	22	80	1½	(110)CuO // (110)Cu	black coating	9

It was observed that the higher the current density the less time was taken for complete oxidation to matt jet black appearance. With lower current density, the epitaxial growth of Cu_2O with parallel orientation was observed along with random CuO (Fig.7), whereas at higher current densities a pattern appears corresponding to a different orientation. The orientation of this CuO pattern (Fig.9) appears to be (110) compared with the theoretical pattern of (110) orientation, Fig.9a, though the positions of 020 and 021 arcs are slightly up in the pattern of Fig.9. Another feature of this pattern is a strong $\bar{2}02$ arc and also the absence (or probably very faint) of $\bar{1}12$ and 112 arcs. If the anodic oxidation was continued

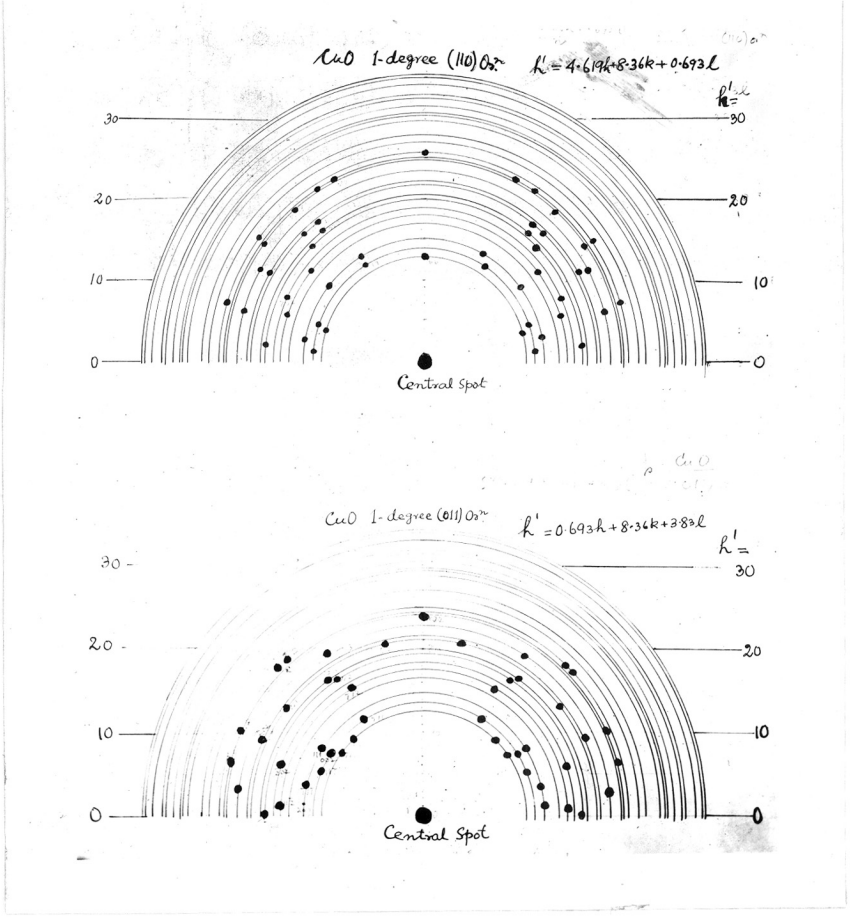

Fig 9a

Fig 9c

Theoretical patterns of CuO, with (110) and (011) orientations

for about 4 mins., the pattern became slightly different (Fig.9b). The orientation appears to be a mixture of (110) and (021), though they have not yet been fully investigated.

The sharp and elongated spots due to Cu_2O in Fig.7 show that the Cu_2O surface was smooth and bounded by a (110) plane mainly. The epitaxial growth of Cu_2O on Cu (110) will be discussed in fuller detail in sub-section (d).

(iii) Effects of Concentration of alkali.

The effects of the concentration of the NaOH solution on the oxidation products as well as on the crystal growth were investigated. The results are shown in Table 3.

Table 3.

Subs.	Conc. % of NaOH soln.	c.d.in ma/cm^2	Temp °C.	Time mins.	Orientation	Appearance	Fig.
Cu(110)	20	10	75±2	6	(110)Cu_2O // (110)Cu $[1\bar{1}0]Cu_2O$ // $[1\bar{1}0]$Cu No formation of CuO	Blue with slight brown tinge	10
Cu(110)	15	6	75±2	6	(110)Cu_2O // (110)Cu $[1\bar{1}0]Cu_2O$ // $[1\bar{1}0]$Cu Twinning of Cu_2O on {111} planes. Traces of random CuO	Bluish	11
Cu(110)	10	6	75±2	6	(110)Cu_2O // (110)Cu $[1\bar{1}0]Cu_2O$ // $[1\bar{1}0]$Cu Random CuO	Brown with black tinge at places.	Similar to 9

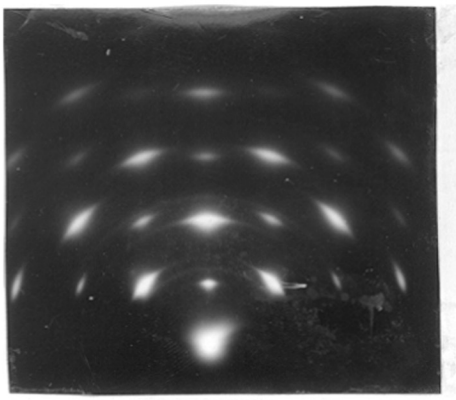

Cu_2O, parallel growth on (110)fac

Beam [001]

Fig 10

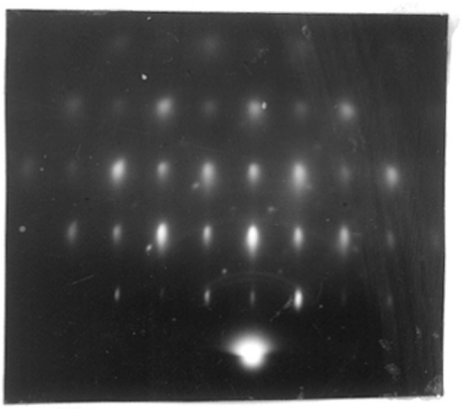

Cu_2O, twinning on {111} planes

Beam [1$\bar{1}$0]

Fig 11

The two-degree orientated pattern of Fig.10 was identified as due to Cu_2O and the measurement of the ring radii are shown in Table 4.

Table 4.

Intensity	Radius in cm.	d spacing in A	hkl planes	a in A.	
s	0.887	3.013	110	4.261	a_o = 4.259 A.
f	1.093	2.460	111	4.236	
s	1.260	2.121	200	4.242	
vs.	1.768	1.512	220	4.276	
vs.	1.974	1.354	310	4.280	

220 Cu = 2.090 cm

λL was calculated from the spacings of 220 Cu spots in Fig.10 and assuming its value to be 1.276 A.

The observed lattice constant for Cu_2O is 4.259 A. compared to 4.252 A. (Wyckoff, 1948). Hence there is no effective change in lattice constant of Cu_2O during the epitaxial growth.

At 20% NaOH, two-degree orientated Cu_2O was formed on Cu (110), with a slight tendency of disorientation. There is no sign of the formation of CuO in the pattern. In Fig.11, the two-degree orientation of the Cu_2O is perfect and the appearance of extra spots in the pattern is due to twinning on $\{111\}$ planes of Cu_2O. This twinning of Cu_2O appears to have been observed for the first time. In Dana's system of

Cu_2O.

Beam along $[1\bar{1}0]$

Fig 12

au773

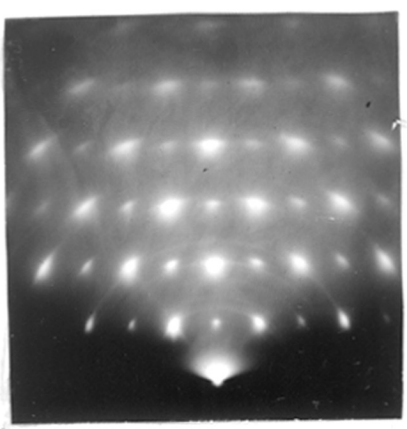

Cu_2O, with facets $\{111\}$

Beam $[1\bar{1}0]$

Fig 13

au768

mineralogy (Palache etc., 1944) there is no reference about the twinning of Cu_2O. The twinned plane was decided from the following considerations.

Diffraction spots due to twinning on hkl type of planes are more prominently observed when the beam is along $\langle 110 \rangle$. The type of twin plane was calculated from the observations of the angle of the rotation of the main spot patterns around the central spot until it coincided with the twin spots. The angle of rotation is given by

$$\theta = 2 \tan^{-1} \frac{\ell}{\sqrt{2}h}$$

If the twin plane is $\{111\}$, then the angle of rotation will be 70°24'. The angle was found to be nearly 71°, hence the twin plane is $\{111\}$ type. Sometimes the diffraction spots due to twinned crystals become more prominent than the main patterns (Fig.12). In these cases it seems that a new orientation is developed in contact with the substrate. Such cases will be dealt with in detail in sub section (d). The patterns shown in Fig.13, obtained also by anodic treatment in 15% NaOH solution shows strong streaks normal to $\{111\}$ planes and to the surface (110) plane. This effect is due to refraction of the electron beams at Cu_2O crystal facets of $\{111\}$ types parallel to the beam or nearly so.

The results in Table 3 show that at about 15-20% NaOH concentration, Cu_2O is formed exclusively, whereas at a lower

Cu_2O, CuO

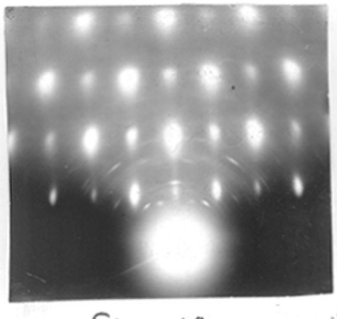

Fig 14
Beam along [110] of Cu (110)

aa 696

Cu_2O, CuO

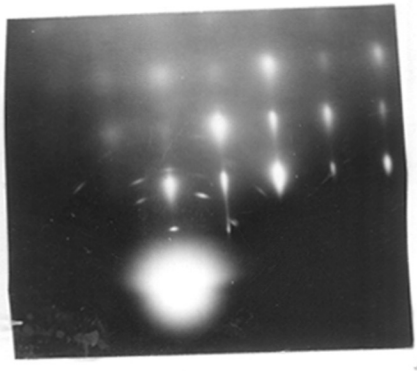

Fig 15
Beam along [001] of Cu (110)

aa 695

Cu_2O, CuO

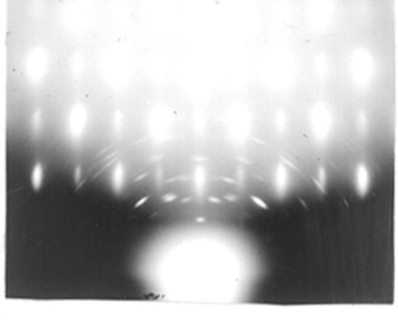

aa 697

Fig 16
Beam along [1$\bar{1}$0] of Cu (110)

Pseudomorphic CuO

concentration, with the same current density, the tendency of CuO formation becomes more and more prominent and results in the formation of one-degree orientated CuO ultimately. At the high concentration of alkali, where two-degree orientated Cu_2O is formed, due to the large lattice constant difference between Cu and Cu_2O (17.7% approx.) a strain will be generated, at the interface, which may probably be relieved either by mechanical twinning, or by disorientation, or by rotational slip. The twinning effect and slight disorientation are seen in Figs. 14 and 10. The rotational slip process will be dealt with in sub-section (d) later.

During anodic oxidation of Cu (110) in 15% NaOH solution at 80°C., in addition to two-degree orientated Cu_2O another two-degree orientated compound was obtained, the lattice constants of which corresponded nearly to normal CuO, with its one axis twice the 'b' spacings of the normal CuO, and with β nearly about 90°. The patterns obtained from this are shown in Figs. 14 and 15. The main patterns are due to two-degree orientated Cu_2O. The short arcs are due to the formation of a new compound. In the $\langle 1\bar{1}0 \rangle$ azimuth of copper (110), Fig.14, two sets of parallel spot rows (Laue zones) perpendicular to each other are seen, the spacings of which are found to correspond to 4.73 A. and 6.954 A. These rows of spots are more prominent in Fig.16. The spacings were

calculated from λL obtained from the diffraction spots due to Cu_2O, the cube axis of which was assumed to be the normal value, 4.252 A. It was already shown ~~that~~ from the measurement of the spot patterns of Cu_2O, Table 4, that in epitaxial overgrowth, the Cu_2O retained effectively its normal dimension. This was also confirmed from the measurement of the CuO ring radii and finding the lattice constant of Cu_2O in Fig.7. The lattice row spacing parallel to the horizontal rows in the 90° azimuth of Fig.[illegible] parallel to the shadow edge was found to be 5.14 A., which corresponds closely to the spacing of the normal CuO. The compound thus formed has therefore the lattice axial dimensions a = 4.73 A, b = 6.95 A, c = 5.14 A., with β = 90° or practically so.

In the normal CuO, the dimensions are a = 4.653 A., b = 3.410 A., c = 5.108 A., β = 99°29' (Tunnell and co-workers, 1935). It appears that the compound formed is also (at least approximately) CuO with slight modification of structure such that its a and c axes are close to the a and c of CuO but its b axis is approximately double that of the b axis of the normal CuO.

This may be a case of pseudomorphism such as first observed by Finch and Quarrell (1933,34) in the case of thin films of ZnO on Zn. The orientation of this pseudomorphic CuO is (120), which corresponds to (110) orientation of the normal

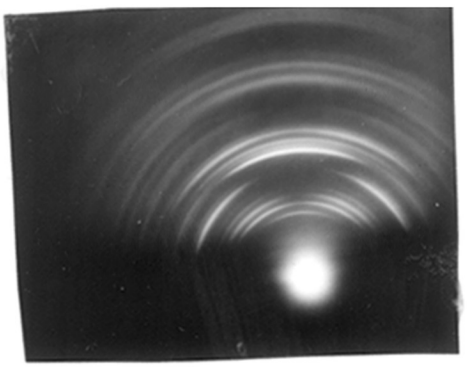

4u 791

Fig 17

Anodically oxidised Cu(110) at 18°C.

CuO. Hence (120) of the pseudomorphic CuO is parallel to Cu (110). Similar pseudomorphic CuO was also obtained by immersing Cu (110) in hot 10% NaOH solution.

The presence of very faint rings as well as the arcing of the diffraction spots due to cupric oxide suggests that the crystals had a tendency to disorientate in all possible directions.

iv. Anodic oxidation at room temperature.

Electropolished Cu (110) was also oxidised at 18°C, with 10 ma./sq.cm. for 2 mins. A greenish coating appeared over the surface. The specimen yielded the pattern shown in Fig.17. The pattern appears to be similar to the normal CuO pattern, though all the rings could not be thus accounted for. A similar pattern was also obtained by Lamchen (1937) by anodic treatment of polycrystalline copper in 20% NaOH solution with 15 ma./sq.cm.

b. Anodic Oxidation of Cu(100), Polycrystalline Copper and Brass.

Copper (100) and polycrystalline copper and brass were anodically oxidised at 80°C. with 10 ma./sq.cm. for 5 minutes till a black coating appeared over the surface. The results are shown in Table 5.

Table 5.

Substrate	Temp °C.	c.d.in ma/sq. cm.	Time mins.	Orientation	Appearance
Cu(100)	80	10	5	(021)CuO // substrate	Black
Cu(Poly)	80	10	5	(021)CuO // substrate	Black
Brass(Poly)	80	10	5	(021)CuO // substrate	Black

In all these cases the patterns obtained were similar to the pattern obtained on Cu (110) surfaces, under similar conditions, as in Fig.4. Thus it is evident that whatever the surface of the substrate the final coating is one degree orientated CuO. It is interesting to note that even brass after anodic oxidation produces CuO (~~Fig.17c~~) closely similar to that on the copper single crystal. The substrate did not show any effect on the orientation of CuO in thick deposits.

c. Anodic Oxidation of Cu (110) in Acid Solution.

A Cu (110) face was anodically treated in HCl solution at different current densities. The results are shown in Table 6.

By anodic treatment in the HCl solution the surface of Cu (110) became rough due to etching and a sheen due to small facets appeared on the copper surface. Fig.19 shows copper spots together with spotty rings passing through the

Displacement of spots

Beam along [1$\bar{1}$0] of Cu (110)

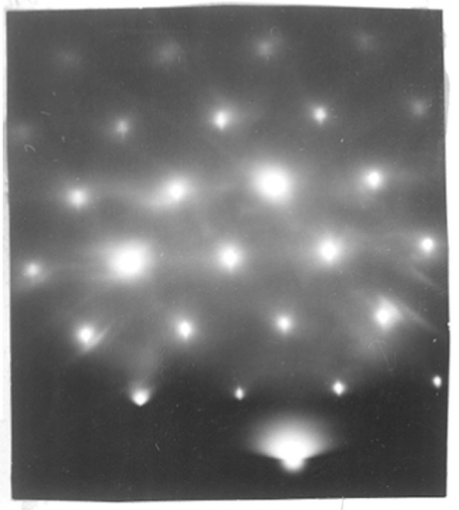

Fig 18 a

Beam along [00$\bar{1}$] of Cu(110)

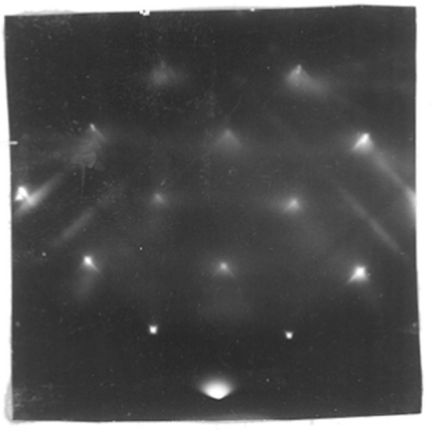

Fig 18 b

Strong refraction effects

Fig 19

Partial disorientation of Cu (110) surface by anodic treatment.

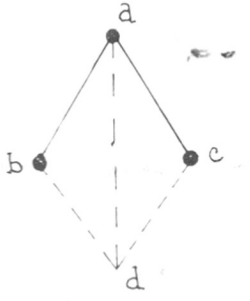

Displacement of spots

FIG. 20(a)

FIG. 20(b)

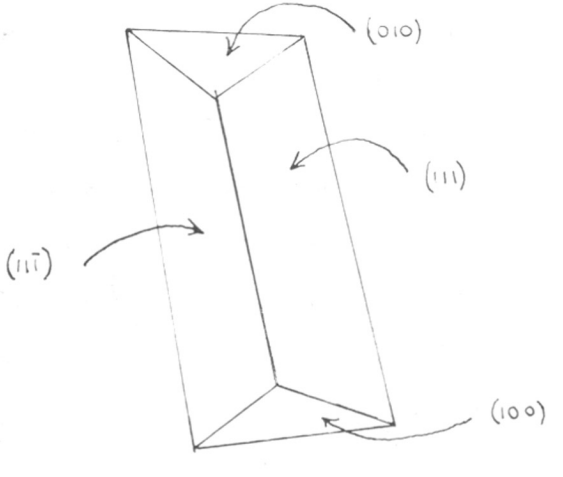

FIG. 21

Facets formed during anodic treatment in HCl soln.

Table 6.

Substrate	Conc. of HCl solution	c.d. in ma/sq. cm.	Time mins.	Fig.	Results.
Cu(110)	16%	10	2	18a 18b	Strong refraction effects on spot patterns of Cu
Cu(110)	32%	90	5	19	Spotty ring pattern of Cu along with the usual spot pattern.

normal diffraction spots of Cu. This indicates that the initial substrate, which was atomically smooth and perfect, became disorientated owing to the vigorous anodic treatment.

An interesting feature is shown in Figs. 18a and 18b. It is seen that most of the spots are not only elongated towards the shadow edge but are also drawn out obliquely like spikes and two distinct spots can be seen (Fig.18a) on the spikes, as in Fig.20a.

These spots correspond to the displacement of the normal spots along a direction perpendicular to $\{111\}$ planes. It seems therefore that the habit of the anodically treated copper surface is such that the crystal projections were bounded by two predominantly octahedral planes (111) and $(11\bar{1})$. The patterns (Fig.18b) in the 90° azimuth also show strong oblique diffraction effects along directions normal to the $\{100\}$ planes. From the strong refraction effects normal to

{111} and {100} planes together with displacement of the spots due to refraction by {111} planes it appears that facets which are bounded by (111), (11$\bar{1}$), (100) and (010) planes are formed by anodic treatment in HCl solution, Fig.21.

Due to the inner potential the beam is refracted when it enters the {111} surfaces at grazing incidence. The appearance of the displaced spots is explained in the following way.

i). If the beam penetrates into the crystal through the front cube-face surface and leaves from the back without any appreciable refraction, the spot position will be at 'a' (Fig.20a) effectively in the normal position.

ii). If the beam penetrates through the plane A with refraction and leaves through the back surface without refraction, the normal spot will be drawn to 'c'.

iii). If the beam penetrates through the front surface (100) and leaves through B with refraction, the spot will be drawn to 'b'.

iv). If the beam penetrates through the plane A and then leaves through B, the spot will be drawn to a position 'd' (which could not be found in the present case).

From the displacement of the spots, the inner potential of the crystal for the faces {111} was measured, after Miyake (1938), as follows.

$$V_0 = 2E.\Delta\phi.\phi$$

where V_0 = inner potential of the crystal face in volts.

$\Delta\phi$ = angular displacement of spots.

ϕ = deviation of the beam from the zone axis where the two main refracting planes meet. Angle of grazing incidence on the facets (i.e. between the beam and the surface)

E = voltage used.

Experimental result.

E = 49 KV. L = 46 cms.

$\Delta\phi$ = .072/49

ϕ = 2.5/49 1.55

$V_0 = 2E.\Delta\phi.\phi$ = 7.9 volts. 5.46

Hence the inner potential of the Cu (111) surface is of the order of 8 volts. 4.5

A similar displaced spot pattern due to inner potential was also observed by Miyake (1938) from octahedral Sb_2O_3 crystals on oxidised stibnite, and he estimated that the inner potential of the Sb_2O_3 was 17 ± 2 volts.

d. Oxidation of Cu (110) and Cu (100) faces by Immersion in Alkaline Solution and Water.

Cu (110) and Cu (100) faces were oxidised by immersion in 10% NaOH solution at different temperatures. The results are shown in Table 7.

Table 7.

Substrate	% of NaOH soln.	Temp. °C.	Orientation	Appearance.	Fig.
Cu(110)	10	75	$(110)Cu_2O$ // $(110)Cu$ $[1\bar{1}0]Cu_2O$ // $[1\bar{1}0]Cu$	Bluish	22a 22b
Cu(110)	10	75	$(114)Cu_2O$ // $(110)Cu$ $[110]Cu_2O$ // $[1\bar{1}0]Cu$ Twinning of Cu_2O on $\{111\}$ planes.	Bluish	23
Cu(110)	10	20	$(110)Cu_2O$ // $(110)Cu$ $[1\bar{1}0]Cu_2O$ // $[1\bar{1}0]Cu$	Brownish	24a ~~24b~~
Cu(100)	10	75	a. $(100)Cu_2O$ // $(100)Cu$ $[011]Cu_2O$ // $[011]Cu$ b. $(221)Cu_2O$ // $(100)Cu$ $[1\bar{1}0]Cu_2O$ // $[011]Cu$ Twinning of Cu_2O on $\{111\}$ planes.	Reddish brown	25a ~~25b~~
Cu(100)	10	20		Brownish	26

Beam along [001]

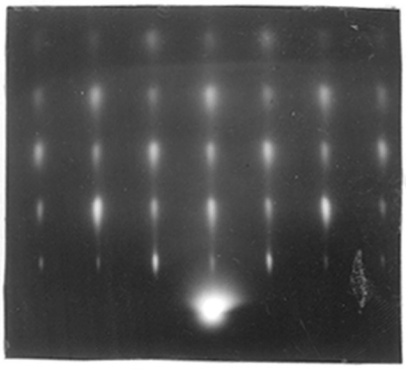

Fig 22 a

(110) orientation

Beam along [1$\bar{1}$0]

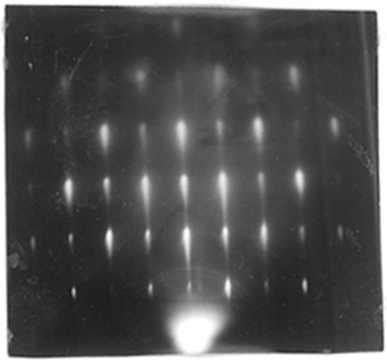

Fig 22 b

(110) orientation

Beam along [1$\bar{1}$0]

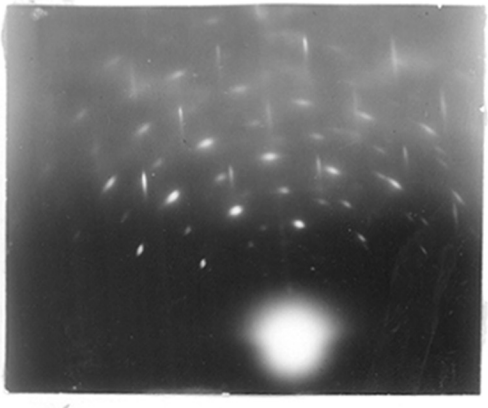

Fig 23

(114) orientation

Beam along [001]

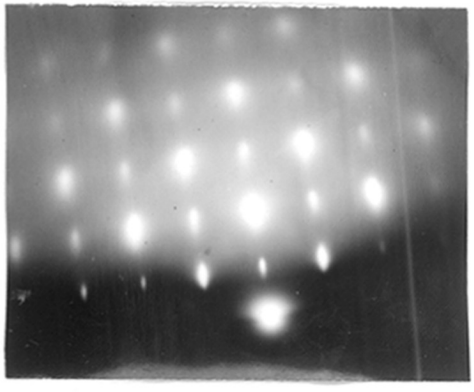

Fig 24a

(110) orientation

Cu_2O on Cu (110)

(2 2 1) orientation

Beam along [1 1 0]

Fig 25a
formed at 45°C

Au 1088

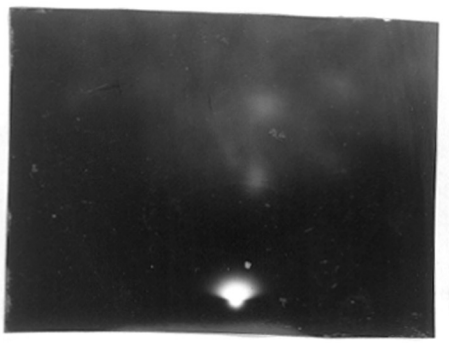

formed at room Temperature

Fig 26

Au 1091

Cu_2O on Cu (100)

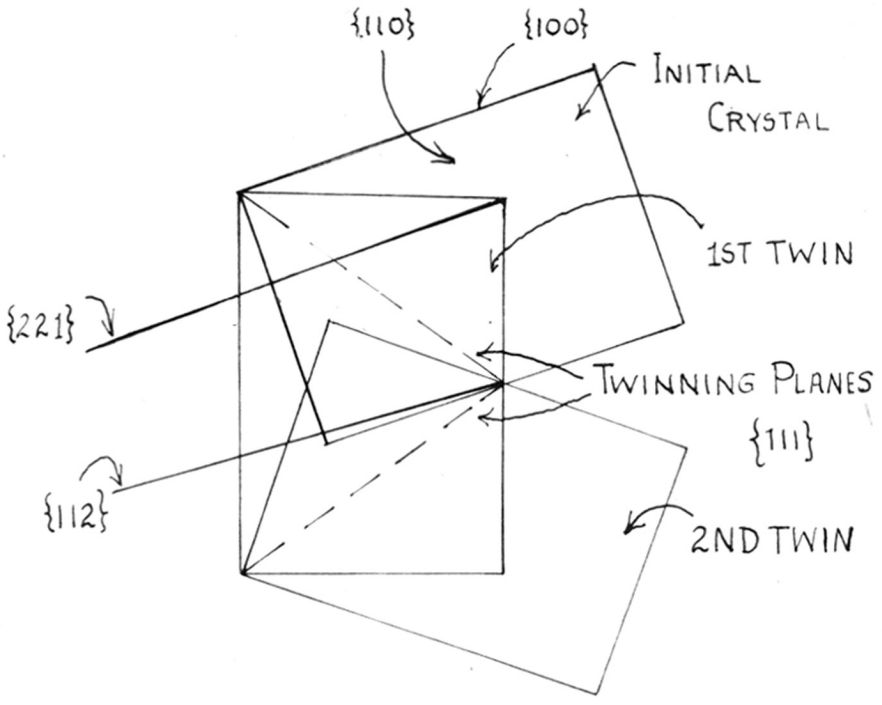

FORMATION OF A TWINNED CRYSTAL

Fig 27

Second twin of Cu_2O.

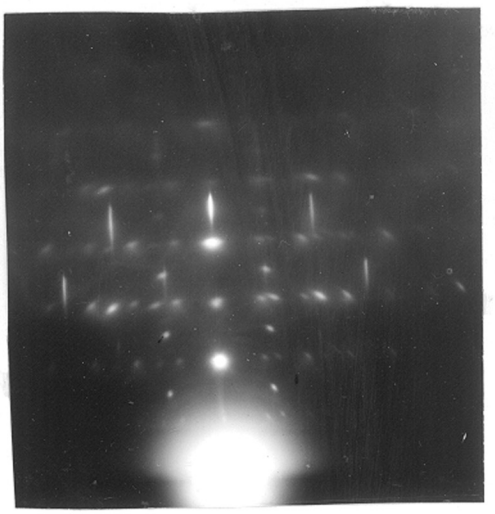

Beam along
[1$\bar{1}$0]

Fig 28a

GU1117

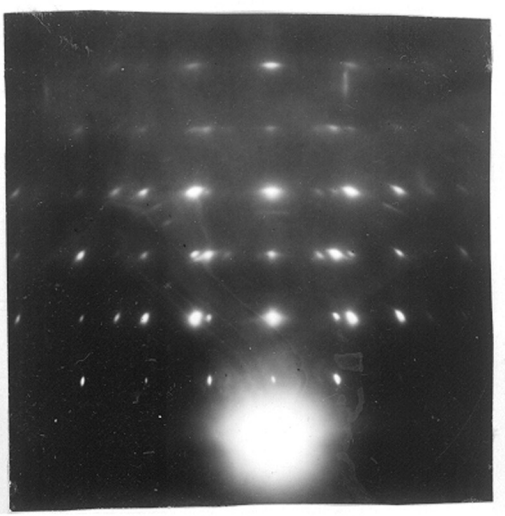

Beam along
[001]

Fig 28b

GU1116

Cu_2O on Cu(110)

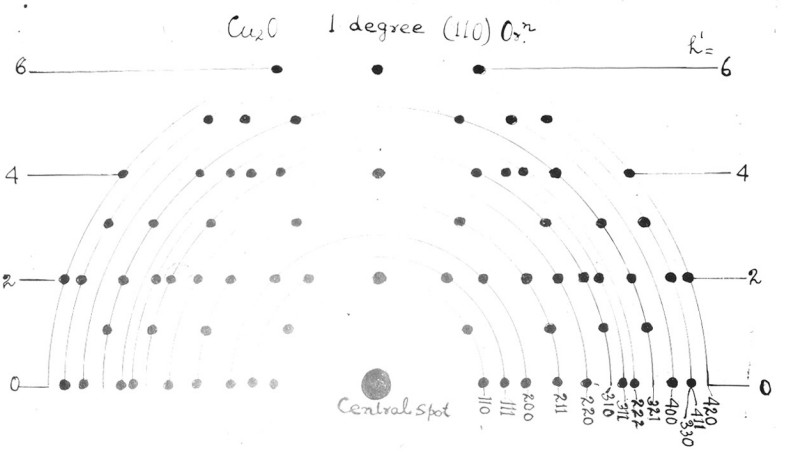

Fig 29

Theoretical patterns of Cu_2O with (110) orientation.

The oxidation product of Cu in alkaline solution was mainly two-degree orientated Cu_2O, though in some cases traces of CuO were observed. The orientation of the Cu_2O on Cu (110) was mainly (110) and sometimes (114) orientation also developed Twinning occurred on $\{111\}$ planes and sometimes it was so prominent as to suppress the diffracted spots due to initial parallel orientation. (Fig.23). The development of (114) orientation on Cu (110) is due to $\{111\}$ twinning as shown in Fig.27. At first, Cu_2O grew with its cube axes parallel to those of the Cu, i.e. (110) Cu_2O parallel to (110) Cu and a cube edge of Cu_2O was along the cube edge of Cu. As the film thickens, due to twinning of Cu_2O on $\{111\}$ planes, a new plane i.e. (114) becomes parallel to the surface and hence (114) orientation develops. In the pattern, Fig.23, some arcing is also observed, which shows disorientation during the crystal growth.

An interesting pattern of Cu_2O on Cu (110) is shown in Fig.28a. The pattern was taken on the same specimen and in the same azimuth as Fig.23, though at a different portion of the specimen. The sharp and elongated spots show that the surface was atomically smooth. The formation of layer lines suggests that the coating of Cu_2O was one-degree orientated, though the pattern in the other 90° azimuth (Fig.28 b) indicates a two-degree orientation of Cu_2O. In order to decide the

degree of orientation, a theoretical pattern of Cu_2O with (110) orientation is drawn (Fig.29) and compared with the pattern (Fig.28a). Though the general features of the patterns Figs. 28a and 29 are similar, there are some discrepancies. The general asymmetry of the spacings of the spot patterns, the position of the spots not being exactly on layer lines (Fig.28a) as well as the absence of a spot in the fourth layer line where it intersects the first row line in Fig.29, shows that the pattern in Fig.28a is not due to one-degree orientation of Cu_2O. The alternative tentative explanation is that the pattern is due to the re-twinning of Cu_2O on $\{111\}$ planes. Due to the double twinning, the original $[1\bar{1}0]$ becomes very nearly $[111]$ of the second twin. Fig.27 shows the formation of the second twinned crystal.

The oxidation of Cu (110) surfaces at room temperature by immersion in 10% NaOH solution also produces two-degree orientated Cu_2O. The pattern is shown in Fig. 24 a ~~and b.~~ Sharp and elongated spots show that the Cu_2O crystals are atomically smooth. Cu_2O grows with parallel orientation on Cu (110).

The Cu (100) face was also oxidised to Cu_2O by immersion in alkali at 75°C. The orientation of the Cu_2O on Cu (100) was (221). The orientation was decided from consideration of the spot patterns of Cu_2O, relative to the

copper spots, which determined the azimuth. The sharp rows of spots along the horizontal lines are due to Cu_2O along [011] and the row of spots nearly normal to the shadow edge is due to rows [111]. The angle between the rows of spots in the plane of incidence and [111] is about 9°. This measurement agrees well with (221) orientation, considering that the initial surface of Cu was about 4-5° off from the (100) face. The development of (221) orientation is again caused by the {111} twinning. Initially probably Cu_2O was growing with parallel orientation on the Cu (100) face, as it does on the Cu (110) face, and then probably due to mechanical twinning on {111} planes, the twin crystals are formed and continue to grow prominently, with (221) planes parallel to the initial Cu surface.

The Cu_2O formed on Cu (100) at room temperature in 10% NaOH solution shows a two-degree orientated rather diffuse spot pattern probably due to the formation of very small crystals. The pattern appears to be similar to the orientation of Ag on Cu (100) by displacement, which will be discussed in Section III. A further study of the formation of Cu_2O at room temperature on an exact cube face of Cu will be useful to settle the orientation of the Cu_2O.

The results of the oxidation of Cu (110) and Cu (100) faces by immersion in water are shown in Table 8.

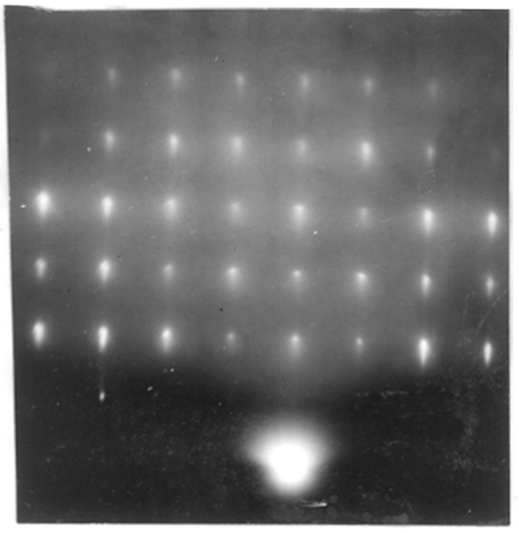

GA 748

Fig 30

Cu_2O in boiling water, on Cu (110) face, for 3/4 hr.

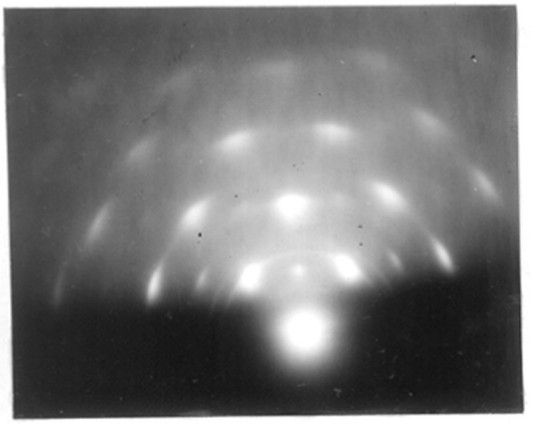

GA 755

Fig 31

Cu_2O on Cu (110) at room temperature for 14 hrs in water

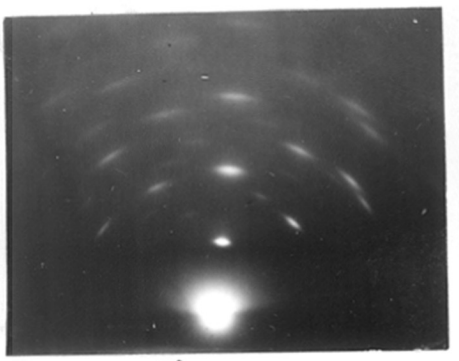

Fig 32a

Cu_2O formed in boiling water in 3/4 hrs on Cu (100) face

Beam along [001]

GA 1128

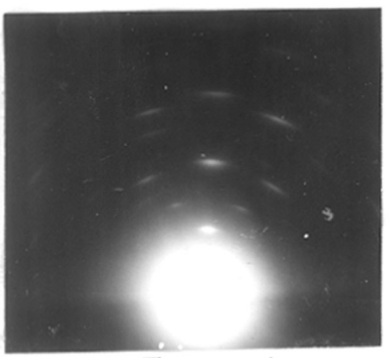

Fig 32b

Beam along [011]

GA 1120

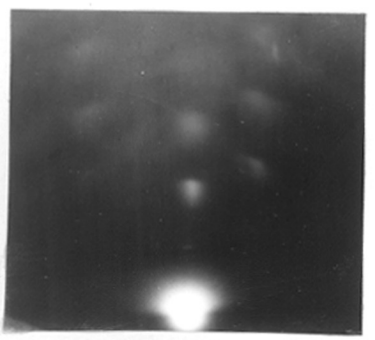

Fig 33

Cu_2O formed in water at room temperature in 14 hrs on Cu (100) face

Beam along [001]

GA 1119

Table 8.

Substrate	Temp. °C.	Time hrs.	Orientation	Fig.
Cu(110)	100	3/4	(110)Cu_2O || (110) Cu $[1\bar{1}0]Cu_2O$ || $[1\bar{1}0]$ Cu	30
Cu(110)	20	14	(110)Cu_2O || (110) Cu $[1\bar{1}0]Cu_2O$ || $[1\bar{1}0]$ Cu	31
Cu(100)	100	3/4	. . . . .	32a 32b
Cu(100)	20	14		33

On Cu (110), again Cu_2O grows with its cube axes parallel to those of the Cu, though there is not much sign of twinning. The patterns (Figs. 3[illegible] and 30) due to Cu_2O formed in water at room temperature and at 100°C. are quite sharp, showing that the crystals were several hundred angstroms in diameter. On Cu (100), Cu_2O was formed in boiling water with (111) plane nearly parallel to Cu (100) (Figs. 32a and 32b). The pattern (Fig.33) of Cu_2O on Cu (100) at room temperature was similar to those obtained by treating in NaOH solution at room temperature (Fig.26). The diffuseness of the spots shows that the crystal size of the oxide formed is very small. The behaviour of Cu (100) in its oxide crystal formation is a

Cu_2O

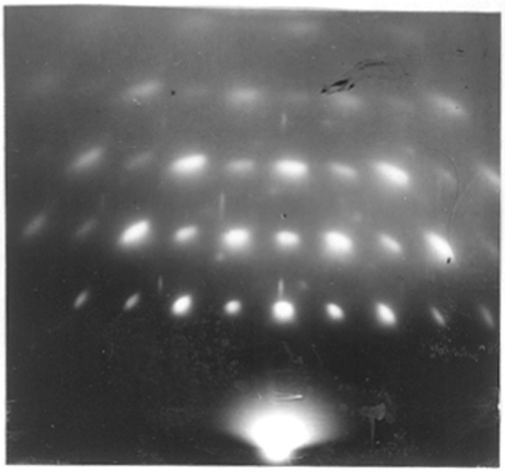

Beam along
[1$\bar{1}$0]

Fig 34a

Au 1087

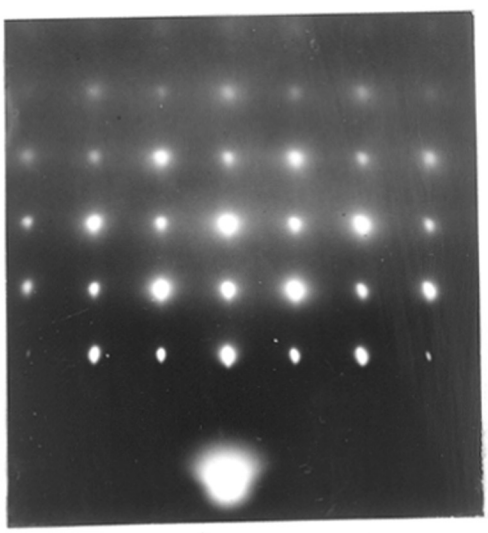

Beam along
[001]

Fig 34.b

Au 1088

Rotational slip of Cu_2O on
{110} planes

striking contrast to that of Cu (110) in water or alkali solution at room temperature.

A new case of relief of epitaxial strain by "rotational slip" (Wilman, 1950) was observed in the case of Cu_2O on Cu (110). The patterns obtained by treating Cu (110) in alkali at about 75°C., are shown in Figs. 34a and 34b along $\langle 1\bar{1}0 \rangle$ and $\langle 001 \rangle$ azimuths of Cu (110). The patterns are due to Cu_2O. Along $\langle 1\bar{1}0 \rangle$ there is considerable arcing of the diffraction spots, whereas in the $\langle 001 \rangle$ azimuth, there is practically no sign of arcing. This suggests the disorientation of Cu_2O by rotational slip on a plane ~~xxx~~ normal to the rotation axis $[1\bar{1}0]$ on (110) planes. Similar rotational slip has also been observed, though more prominently, in the case of Cd on Cu(110) and will be described in Section II. Recently Evans and Wilman (1950) have ~~also~~ observed such a rotational slip in the formation of ZnO on ZnS (110) by heating in air. Due to large lattice difference between Cu_2O and Cu (17.7% approx.) a stress is generated on or near the Cu_2O-Cu (110) interface. As the Cu_2O film thickens, the stress will increase and ultimately it may be relieved by a mechanical twinning or recrystallisation or rotational slip process. In this case the strain was relieved by rotational slip.

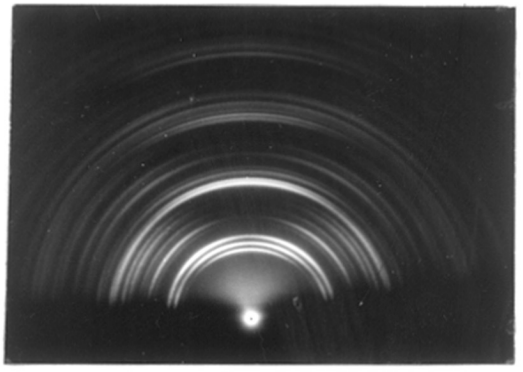

Fig 35 Fig~

CuO formed in air at 400°C.

e. Oxidation of Polycrystalline Cu in Air.

Polycrystalline copper was oxidised in air by placing it on a heated metal block at about 400°C. for 30-60 seconds. Fig.35 shows the pattern of CuO so obtained. The pattern shows an orientation different from those obtained by anodic oxidation process (Fig.4). The orientation was determined from a comparison with theoretical patterns, Figs. 5, 6 and 9a and found to agree mostly with (110) orientation, though the position of $20\bar{2}$ arcs is slightly low down and the 020 arc is slightly high up in the theoretical pattern, compared with the observed pattern (Fig.35).

f. Halide on Cu (110) Surface.

$CuCl_2$ and Cu_2Br_2 were prepared by exposing Cu (110) surface to Cl_2 or Br_2 vapour in presence of air, by anodic or chemical treatments. A bath containing 10 g./l. NaCl and 25 cc./l. of HCl was used for Cu_2Cl_2 preparation by anodic treatment. A bromide bath of composition 5 g./l. NaBr and 25 g./l H_2SO_4 (conc.) was used for anodic or chemical treatment. Attempts were made mainly for the preparation of two-degree orientated cuprous halides. The results are shown in Table 9.

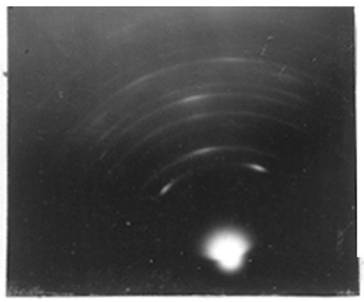

Fig 36a

au 949

Cu_2Cl_2 in chlorine vapour

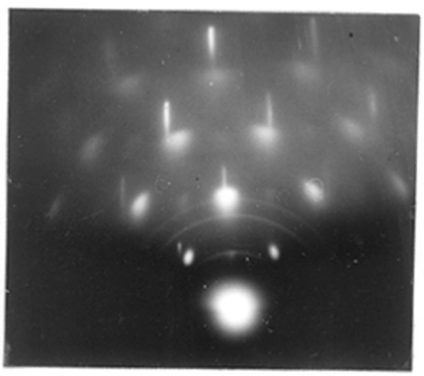

Fig 37

au 861

Cu_2Cl_2 and Cu_2O, by anodic treatment

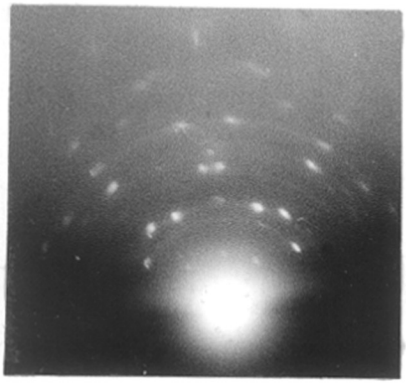

Cu_2Br_2 formed in 10 sec anodically

(111) orientation

GL 964 Fig 38

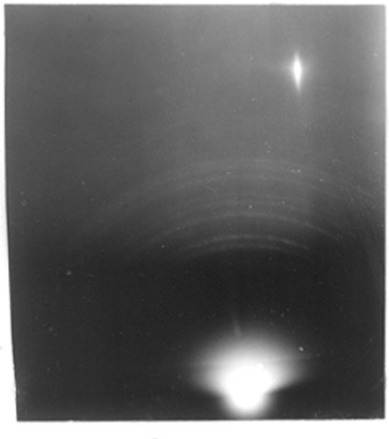

Cu_2Br_2 formed in 20 sec anodically

Random

GL 962 Fig 39

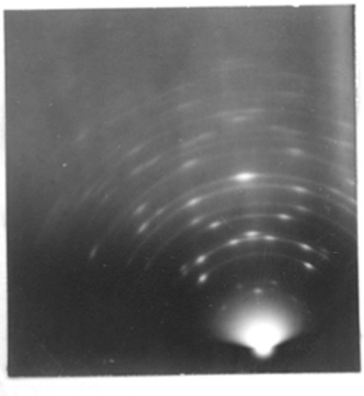

Cu_2Br_2, dry immersion

(111) orientation

GL 967 Fig 40

Table 9.

Substrate	Treatment	Orientation	Fig.
Cu(110)	Cl_2 vapour for 5-10 secs.	(311) and (211) planes parallel to the surface	36a
Cu(110)	Anodically treated in chloride soln. for 1 min. at 4 ma./sq.cm.	two-degree orientated Cu_2O (Parallel growth) and random Cu_2Cl_2.	37
Cu(110)	Anodically treated in bromide soln. for 10 secs. at 2.1 ma./sq.cm.	two-degree orientated Cu_2Br_2. $(111)Cu_2Br_2 // (110)Cu$ $[1\bar{1}0]Cu_2Br_2 // [1\bar{1}0]Cu$	38
Cu(110)	As above for 20 secs.	Twinning on {111} planes.	
		Random	39
Cu(110)	Immersion in bromide soln for 10 secs.	two-degree orientation $(111)Cu_2Br_2 // (110)Cu$ $[1\bar{1}0]Cu_2Br_2 // [1\bar{1}0]Cu$ Twinning on {111} planes	40

In all the experiments Cu_2Cl_2 obtained was either random or one-degree orientated (Figs.36a and 37). Cu_2Br_2 grows with (111) plane parallel to (110) of Cu and the twinning planes are {111}. Usmani (1941) also observed similar twinning of Cu_2Br_2 on {111} planes, working with Cu (111) face.

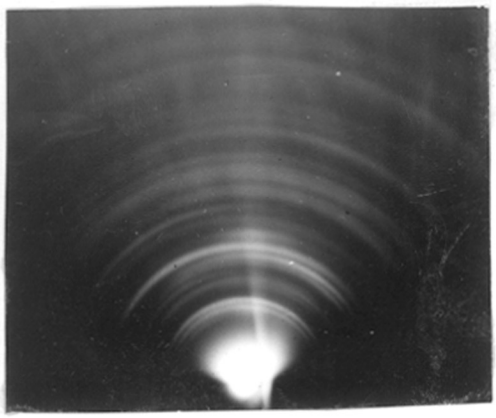

Beam perpendicular to the rubbing direction

Fig 41

Gu 35

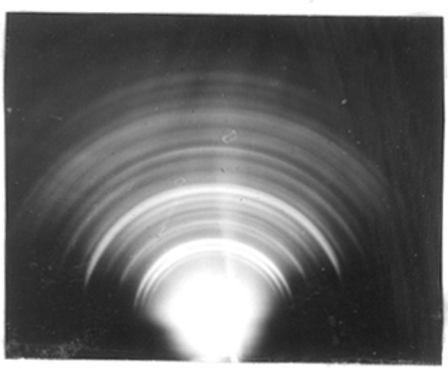

Beam along the rubbing direction

Fig 42

Gu 36

Ceo patterns after unidirectional rubbing

Asymmetric Pattern of Cupric Oxide after Unidirectional rubbing

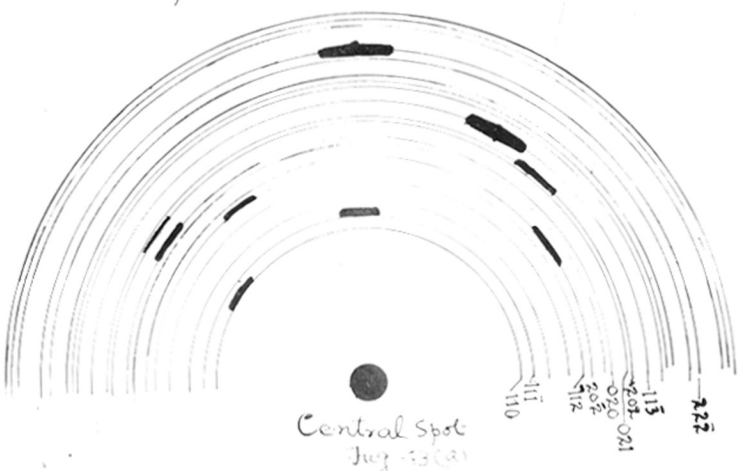

Fig 43a

Cupric Oxide Cell and rubbing direction

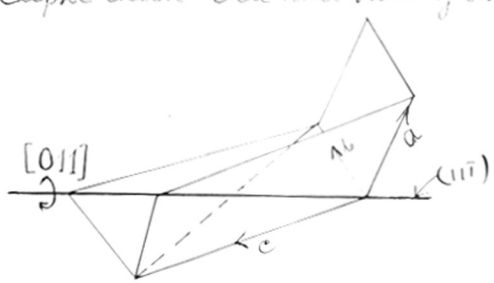

Fig 43(b)

Fig 43b

In anodic treatment, when the time of treatment was about 10 secs., two-degree orientated Cu_2Br_2 was formed (Fig.38a) but when the time of treatment was about 20 secs., the pattern becomes random (Fig.39). This shows that Cu_2Br_2 which was growing epitaxially was transformed into random disposition with thickness of the coating. The epitaxial growth of Cu_2Br_2 simply by immersion is also shown in Fig.40.

g. Effects of Unidirectional Rubbing of CuO formed anodically.

An interesting new phenomenon was observed when a polycrystalline one-degree orientated CuO obtained by anodic oxidation was rubbed unidirectionally with cotton wool. It was found that the one-degree orientation of CuO similar to Fig.4 was transformed into an approximately two-degree orientation (the second degree of orientation being related to the direction of rubbing) and the matt black surface was simultaneously changed to a polished reflecting one. The specimen yielded asymmetric patterns of arcs (Fig.41) when the beam was perpendicular to the rubbing direction and symmetrical patterns (Fig.42) when the beam was along the rubbing direction.

The shortness of the $11\bar{1}$ and $22\bar{2}$ arcs in the plane of incidence in the asymmetrical pattern together with the

long arcs in the symmetrical pattern shows that the CuO crystals were orientated so that a lattice row in the (11$\bar{1}$) plane was closely parallel to the rubbing direction; but otherwise with considerable disorientation due to rotation about this direction as axis. The asymmetrical pattern thus amounts to a partial rotation pattern about an axis normal to the beam and parallel to the shadow edge.

We may estimate the direction of this rotation axis by a trial and error process as follows. Trying first [101] as rotation axis normal to the beam with an initial crystal orientation such that (11$\bar{1}$) plane is parallel to the specimen surface, a rotation of about 40° is required to bring the (020) plane into the reflecting position, but this plane is then parallel to the surface and would therefore give a Bragg reflection arc in the plane of incidence. This is contrary to the observed pattern (Fig.41). Further evidence of its incorrectness is obtained from the consideration of the diffraction expected from planes such as (110) and ($\bar{1}$10).

If [1$\bar{1}$0] were the rotation axis, then starting from the orientation such that (11$\bar{1}$) plane is parallel to the surface, a rotation of about 20° brings the (110) plane parallel to the surface and it should therefore give a strong arc in the plane of incidence, but it does not. At the same time also a 020 reflection should appear to the left of the plane of incidence

at about 40° from this plane approximately as observed, but a $\bar{1}10$ reflection would occur low down near the shadow edge, and this is not the case. Thus $[1\bar{1}0]$ cannot be the rotation axis.

On the other hand a trial of [011] as rotation axis gives good agreement with the pattern Fig.41, starting from $(11\bar{1})$ plane parallel to the surface. Thus a small rotation brings a $\{110\}$ plane set into the reflecting position and the 110 arc would then be about 34° to the left of the plane of incidence. About 30° further rotation brings (020) plane into the reflection position. This also gives an arc along the same radius as the 110 arc to a good approximation, as observed in Fig.41. Rotation in the opposite direction brings the $20\bar{2}$ plane so as to give a reflection on the opposite side of the plane of incidence, as also $11\bar{3}$ reflection. These expectations also agree with the figure,[43a] and 021 and $\bar{1}12$ reflection should occur on the left side of the plane of incidence, also at the observed positions. The only discrepancy appears to be the occurrence in the pattern of what might be the $20\bar{2}$ arc of medium intensity to the right of the plane of incidence, whereas it should have been on the left, though requiring 90° rotation from the initial orientation taken as $(11\bar{1})$ parallel to the surface.

However a [011] axis of common orientation of the crystal is most in agreement with Fig.41 and it can be readily

explained in terms of the known cleavage planes $\{11\bar{1}\}$ and the usual $\{100\}$ plate and lath habit of CuO (Palache, Berman and Frondel, 1944). Rubbing a layer of CuO having such a $\{100\}$ habit would probably cleave the crystals into lath-shaped fragments, whose length is along [011] and owing to the raking action of abrasive material these laths will tend to align along the abrasion direction, probably with some disorientation about the abrasion direction as axis.

This picture therefore accounts for [011] axis parallel to the abrasion direction, suggested from the diffraction pattern, though it is difficult to see, in this case why an asymmetric pattern is obtained when the beam is normal to the abrasion direction, because the lath shaped fragments could have their length equally well parallel to the rubbing direction or anti-parallel to it. However, this asymmetric pattern has been repeatedly obtained and when the uni-direction -al rubbed surface was further rubbed at right angles to the initial rubbing direction, the same asymmetric pattern was again obtained, in the same way relative to the new abrasion direction. Since translational slip directions of CuO are not yet known it is not clear whether an alternative interpretation in terms of slip is possible.

Similar asymmetric patterns, though less prominent, were also observed from CuO formed by heating polycrystalline Cu in air by unidirectional rubbing.

4. Discussion.

The present experiments go considerably further than the scanty previous knowledge on the anodic crystal growth processes.

It is seen from the above experimental results (Section I, (3), that during the anodic oxidation of Cu in alkaline solution, both Cu_2O and CuO are formed. The preponderance of one or other of these oxides depends upon the conditions of treatment. The formation of two-degree orientated (pseudomorphic), random and one-degree orientated CuO in the different experiments together with the fact that two-degree orientated Cu_2O is formed by immersion in alkaline solution suggests that even in the anodic crystal growth process, initially the CuO crystals tend to grow epitaxially on the Cu_2O surface. This is further confirmed by the initial formation of two-degree orientated Cu_2Br_2 and its transformation into random Cu_2Br_2 with increasing time of treatment. It may thus be suggested that, in the anodic crystal growth process, there are several different stages analogous to those demonstrated by Finch, Wilman and Yang (1947) in the case of the cathodic deposits. In the first stage, the oxygen or halogen combines with the metal to form oxide or halide epitaxially. Depending upon the nature of the substrate and

that of the deposit, the initial orientation tends to be degenerated into random disposition. Finally the deposit crystals will tend to grow preferentially either with a simple net plane parallel to the substrate or a densely populated lattice row normal to the substrate, according to the solution concentration and temperature, which determine the relative importance of the supply of anions to the anode by diffusion or by electrical migration.

The above picture of the anodic crystal growth process probably holds good in the case of the formation of halides by halogen vapours. Thus it may be said that the crystal growth process either in anodic or cathodic deposition is fundamentally the same, with the main difference being that in the anodic process, oxygen combines initially with the anode metal to form oxides but further growth depends on the supply of metal atoms through the anode.

The formation of the oxide or halide film by anodic oxidation can be visualised in the following way.

The first layer of anions adsorbed on the metal combine with it to form a film of the oxide or halide over the metal surface. For the next layer to grow, the metal ions diffuse through this film and combine with the anions and continue the deposition on the previous oxide or halide coating. In this way the film grows in thickness and the

orientation of the film also changes from the epitaxial growth to random and finally to one-degree orientation.

During the epitaxial growth of the Cu_2O on the Cu surface a stress will be generated near the Cu_2O - Cu interface, due to the misfit between the atoms in the deposit and the substrate. With increasing crystal size of the Cu_2O this stress will increase and such a stress may be relieved by mechanical twinning, retwinning of the twinned crystals, rotational slip (Evans and Wilman, 1950; Wilman, 1950), or in some cases flexural translational slip.

In the Cu_2O deposits on Cu (110) a $\{111\}$ twinning (and possibly secondary $\{111\}$ twinning also) and rotational slip on $\{110\}$ planes have been observed in the present experiments.

SECTION II.

CATHODIC CRYSTAL GROWTH.

A. Epitaxial Crystal Growth in Cathodic Deposits.

1. Introduction.

Huntington (1905) observed that the microstructure of copper deposited on a copper base could be influenced by the substrate. Similar observations were also made by Blum and Rawdon (1923) and Graham (1923). Hothersall (1935) made a further study of the cathodic deposits by optical microscopy. He observed that several metal deposits followed the microstructure of the base metal, though they sometimes belonged to different crystal systems. The continuation of the microstructures of the annealed copper, annealed nickel, silver and cast α-brass by copper deposits was observed by him. Tin followed the microstructures of annealed tin and annealed copper. He also noticed that metals belonging to the same crystallographic system should have lattice difference less than 15·2 % if the substrate microstructure was to continue.

The conclusions drawn by these authors about the continuation of the substrate structures are rather misleading because what they observed was the habit of the aggregate of

innumerable crystals formed on the polycrystalline substrates. The crystals growing over the substrates might not follow the substrate at all (in the sense of atomic fitting) and might be random while still possessing a habit in the aggregate crystals similar to that of the base metals. In fact, Finch and his co-workers (1936, 1947) by electron diffraction have shown that under suitable conditions epitaxial crystal growth occurs in electrodeposits, but that the deposit on a single crystal substrate often grows without any relation to the substrate lattice after attaining a thickness of several hundred angstroms.

With respect to deposits on polycrystalline substrates, Wood (1931), by X-ray diffraction, observed that Ni and Cu follow the orientation of a one-degree orientated Cu (110) substrate. Clark, Pish and Weeg (1944) have also observed a definite orientating relationship between Zn and Ni on Cu; Zn on Fe. The substrates were all cold worked polycrystalline metals.

The epitaxial growth of cathodic deposits has been studied by Thomson (1931), Cochrane (1936) and in particular by Finch and his collaborators (1936, 1937, 1947) by electron diffraction. Thomson (1931) observed parallel growth of silver on an etched single crystal of Cu. Finch and Sun (1936) observed the strong influence of the substrate on the cathodic

deposit. They studied the crystal growth on substrates of different nature, such as amorphous and crystalline, one degree orientated or nearly single crystals. Epitaxial crystal growth of many metal deposits were observed by them.

Cochrane (1936) obtained parallel growth of Ag, Ni and Co on an etched single crystal of Cu (110) and Cu (111) at a very low current density. He also obtained two degree orientation with (110) Cr parallel to (111) Cu and cube edge of Cr along the cube face diagonal of Cu. He observed pseudomorphism (first observed by Finch and Quarrell (1933-34) in ZnO on Zn) of Ni on Cu single crystal.

Thirsk (1939), under Professor Finch's supervision, observed epitaxial growth of Au, and Ag on Fe (110) face, when the deposition was carried out at a low current density. He also observed parallel growth of Ag, Ni, Co on approximately (110) and (100) surfaces of Cu. Homes and Maquestiau (1945) also observed epitaxial growth of Cu on Fe (100). Finch, Wilman and Yang (1947) have shown that in the cathodic crystal growth there are three distinct stages. In the first stage the deposit structure and orientation is greatly influenced by the substrate and in the second stage the substrate influence is counterbalanced by the effect of the bath conditions. In the final stage the orientation of the deposit is determined by the bath conditions. They also recorded many cases of epitaxial growth of different metals on various faces of Cu and iron

substrates.

Few cases of two-degree orientated hexagonal metal have yet been reported. Yang (1948) has investigated epitaxial growth of Sb on Sb cleavage face (111) and Sb on (100) and (111) Bi. A study of new cases of epitaxial growth of metals belonging to the hexagonal system will be of great interest. Another aspect of this epitaxial crystal growth is that unless the atomic fit between the two metals is very close, a stress will be generated near the deposit-substrate interface, which might affect the crystal orientation of the deposit on the substrate (Van der Merwe, 1949, Evans and Wilman, 1950).

2. Experimental.

The methods for preparing the Cu (110) and Cu (100) faces have already been described in Section I and hence are not included here.

Electrodeposition procedure:-

The circuit for the electrodeposition was similar to the electropolishing circuit described in Section I.

The bath solution was kept in a beaker of about 250 cc. capacity and it was heated by a bunsen burner over a wire gauze. The temperature of the solution was maintained constant within $\pm$ 2°C. The cathodes were electropolished single crystal copper surfaces, which were coated with collodion so that only the

required surface was kept exposed for electrodeposition. The specimens were held by crocodile clips which were also coated with collodion. The anode and cathode were kept vertically facing each other. The distance between the anode and cathode was about 3 cm. The anodes used were of the same materials as those which were to be deposited on the cathode. In order to minimise the inclusion of impurities, the solutions were electrolysed for about 5-10 mins., using unwanted cathodes, before deposition on to the copper crystal surface. The anodes were also coated with thick deposits of the same metals. The current density was calculated from the known area of the copper surface and the current passed. The composition of the baths used for deposition are given below.

Copper bath.

		grams/litre.
	$CuAc_2\ 2H_2O$	25
	$Na_2SO_3 . H_2O$	50
	KCN	35
	Na_2CO_3	10
Cadmium		
	CdO	32
	KCN	88
Iron		
	$FeSO_4(NH_4)_2\ SO_4\ 7H_2O$	350
	H_2SO_4	25

		grams/litre
Nickel		
	$NiSO_4 \cdot 7 H_2O$	240
	H_3BO_3	30
Zinc		
	$Zn(CN)_2$	48
	KCN	64
	Na_2CO_3	4
Silver		
	AgCN	3.5
	KCN	3.7
	K_2CO_3	3.8
Lead		
a)	PbO	10
	NaOH	78
b)	$Pb(OH)_2, 2PbCO_3$	150
	50% HF	240
	H_3BO_3	105

3. Results.

Fe, Cd and Zn were deposited on (110) and (100) faces of Cu under the conditions of the epitaxial crystal growth. The results and the conditions of the deposition are shown in Table 10. The experiments were repeated several times, and similar results were obtained.

(211) Fe on (110) Cu

Beam along [1T0] of Cu

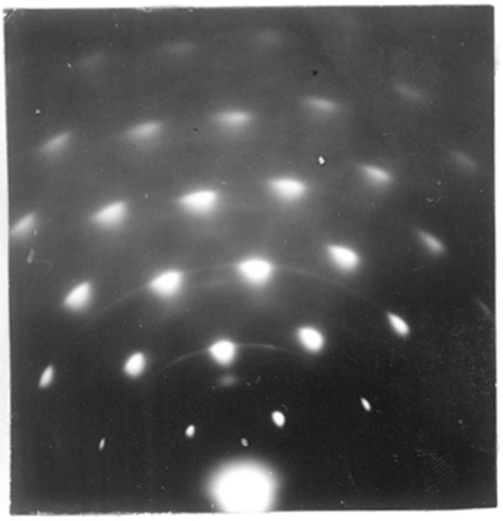

Fig 44a

Beam along [001] of Cu

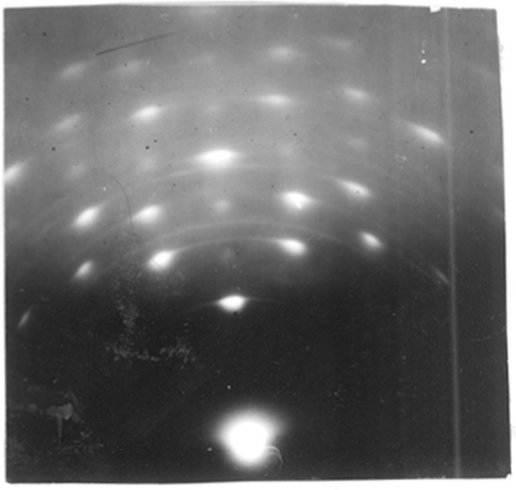

Fig 44b

(110) Fe on (100) Cu

Beam along [01] of Cu

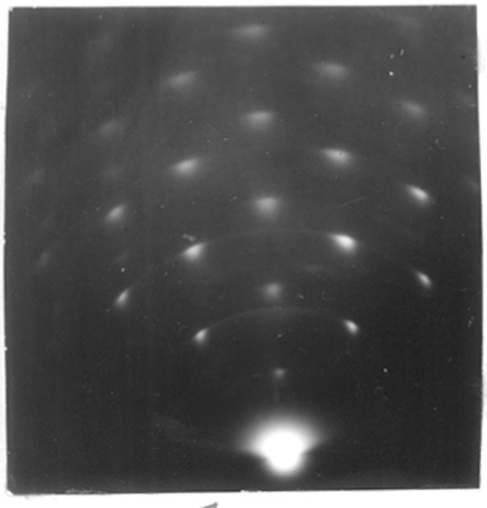

Fig 45a

Beam along [001] of Cu

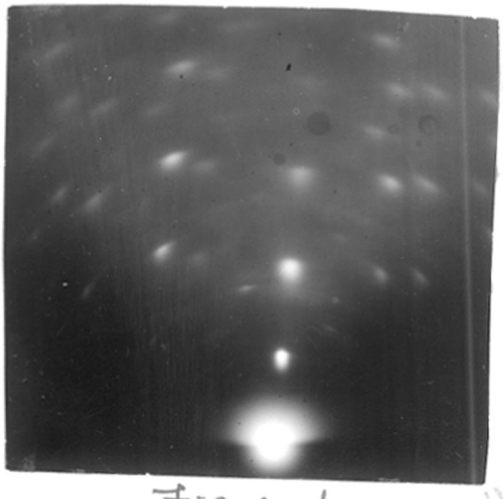

Fig 45b

Fe deposits on Cu

(103) Cd on (110) Cu

Beam along [110]

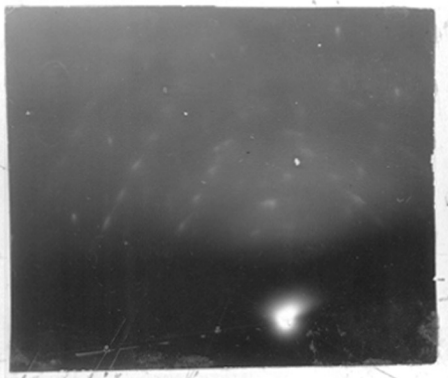

Fig 46a

Beam along [001]

Fig 46b

(203) Cd on Cu(100) tac

Beam along [001]

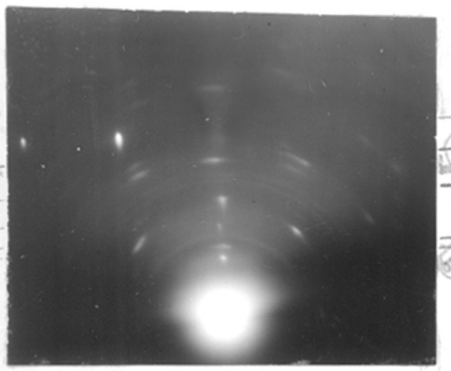

Fig 47a

Beam along [011]

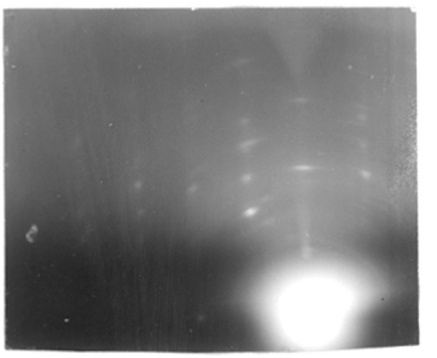

Fig 47b

Cadmium on Copper

Beam along [1̄10]

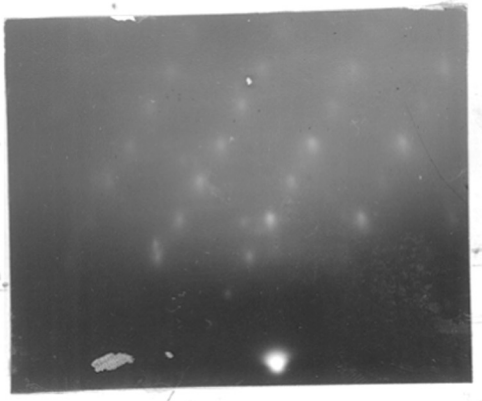

Fig 48 a

Beam along [00]

Fig 48 b

(205) Zn on (110) Cu

Beam along [011]

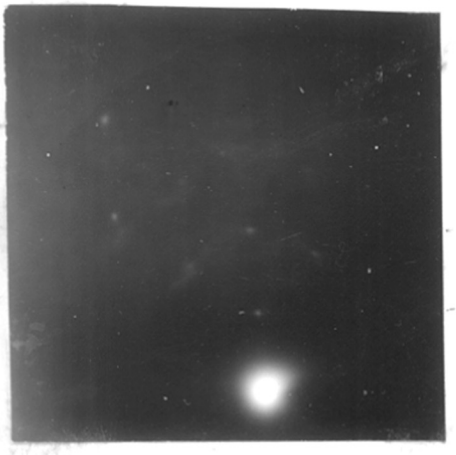

Fig 49 a

Beam along [001]

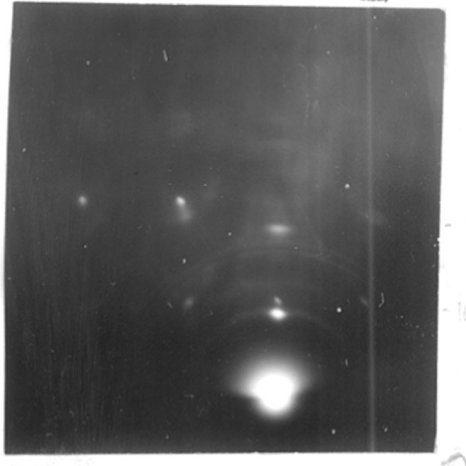

Fig 49 b

(101) Zn on (100) Cu

Zinc on copper

Iron.

Two degree orientated Fe deposits were obtained on Cu (110) and Cu (100) faces and the patterns are shown in Figs. 44a, 44b, 45a and 45b. On the Cu (110) surface, Fe crystals grew with a (211) plane parallel to Cu (110) and the cube face diagonal of Fe along the cube axis of Cu. In Figs. 44a and 44b, in addition to the normal two-degree orientated Fe diffraction spots, there are some additional faint spots due to two-degree orientated oxide of iron, either formed during the deposition of iron, or during the transfer of the specimen to the camera. The lattice constant was estimated to be 8.37 A., assuming the (211) diffracted spot of Fe, which is in the plane of incidence (Fig.44a) to have a spacing of 1.166 A. Hence the oxide is either cubic γ-Fe_2O_3 or Fe_3O_4, the lattice constant of which is 8.37 A. This iron oxide had its (110) parallel to the (211) plane of two-degree orientated Fe on Cu (110).

On the Cu (100) surface, two degree orientated Fe is formed with a (110) plane parallel to the (100) surface of the Cu crystal and the cube diagonal of Fe along the cube face diagonal of the Cu crystal. It is also seen that though the Fe deposits are two degree orientated with respect to the substrate in general, there are some rings passing through the Fe spot pattern. This suggests that though the crystals are

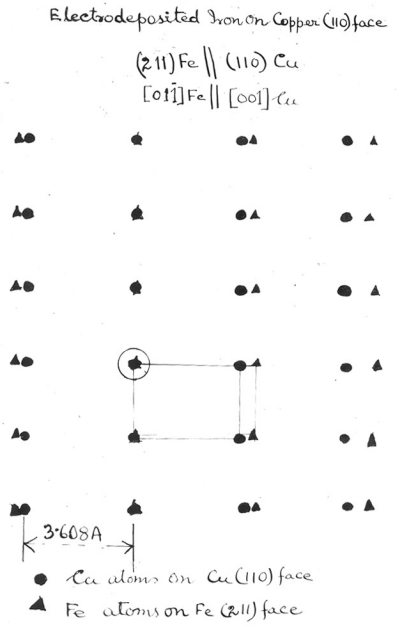

Fig 50

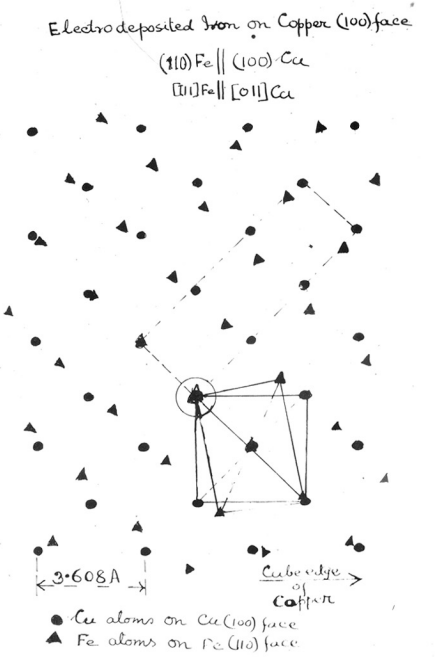

Fig 51

Atomic fitting of Fe on Cu

(0001) $Cd(OH)_2$ // (110) Cu

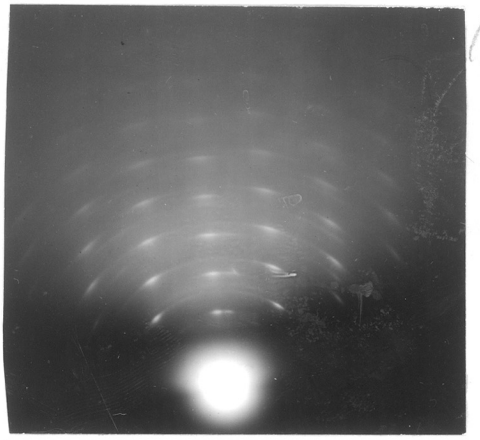

Beam along [1$\bar{1}$0]

Fig 52a

$Cd(OH)_2$ on Cu (110)

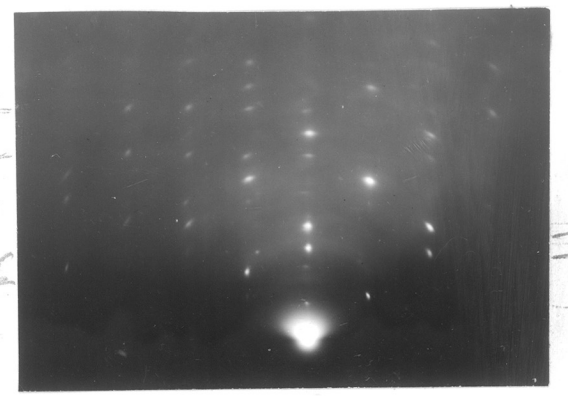

Beam along [00$\bar{1}$]

Fig 52b

$Cd(OH)_2$ and Cd on Cu (110)

Cadmium hydroxide and cadmium on Cu (110)

mainly in two degree orientation, a small proportion of the Fe crystals lie in all possible directions in space, without any relation to the substrate. The atomic and lattice fitting of the Fe on the Cu substrate in their contact planes is shown in Figs. 50 and 51.

Cadmium.

The electron diffraction patterns Figs. 46a and 46b were obtained from the epitaxial growth of Cd on Cu (110) with the beam along Cu [1$\bar{1}$0] and Cu [001] respectively. The two sets of parallel spot rows (Laue zones) perpendicular to each other in Fig.46a are due to the c and a lattice rows of the Cd. The smaller spot separation corresponds to c* of Cd and the other corresponds to a*. The orientation was determined from the spot appearing in the plane of incidence. The 103 diffraction of Cd in the plane of incidence and hence (103) was parallel to the (110) plane of Cu; the [100] row of Cd being along the Cu [1$\bar{1}$0] row. The lattice constant of Cd was also calculated. From the Cu spots in Fig.46b L was calculated and from the horizontal spacing between the vertical spot rows of the Cd the a axis length was found to be 2.974A. which agrees well with the X-ray data 2.973 A. (Wyckoff, 1948). The length of the c axis was also calculated from the pattern Fig.46a, and was found to be 5.55 A., which also agrees well with X-ray data 5.607 A. (Wyckoff, 1948). The deposition of

Cd on Cu (110) was also tried from room temperature to at 75°C. In all cases the (103) of Cd was found to be parallel to (110) of Cu.

A special feature of the pattern of (103) orientation of Cd on Cu is that when the beam was along [1$\bar{1}$0] direction of Cu (110), the pattern showed strong arcing, (Fig 46a) whereas in the 90° azimuth, i.e. along [001] of Cu, there was much less arcing and the spots were sharp. This shows that the Cd deposit crystals were slightly disorientated by rotation about an axis parallel to [1$\bar{1}$0] of Cu. In the (103) orientation of Cd this rotational slip thus occurs on planes which are normal to this rotation axis, i.e. on $\{11\bar{2}0\}$ planes of the Cd. This disorientation on $\{11\bar{2}0\}$ is due to the stress caused near the deposit-substrate interface due to the misfit in the atomic positions of the deposit crystals and those of the substrate. This is the first instance, so far known, of the relief of epitaxial stress by rotational slip in electrodeposits. Similar relief of epitaxial stress by rotational slip has also been observed by me in the case of Cu_2O on Cu (110) (see Section I) and such slip was first observed by Evans and Wilman (1950) in the case of ZnO formed by heating ZnS (110) surfaces.

During the deposition of Cd on Cu (110) in one case, at 75°C., the epitaxial growth of $Cd(OH)_2$ on Cu (110) was also

observed. The patterns obtained along [1$\bar{1}$0] of Cu are similar to Fig.52a. In the other main azimuth, [001], the pattern Fig.52b shows not only $Cd(OH)_2$ but also the normal pattern of Cd.

The $Cd(OH)_2$ (Hexagonal, a = 3.47 A., c = 4.64 A.) had (0001) parallel to Cu (110) and [100] of $Cd(OH)_2$ was along the cube face diagonal of the Cu.

The patterns from the epitaxial growth of Cd on the Cu (100) face are shown in Figs. 47a and 47b. The strong 203 diffraction in the two azimuths ([001] and [011] of the Cu) lies in the plane of incidence, thus the orientation is (203). In addition to the (203) orientation, some (0001) orientation of Cd was also shown by Fig.47b. The vertical rows of diffraction spots in Fig.47b show that the (0001) of Cd was parallel to the Cu (100) surface and [100] of Cd was along the cube face diagonal of the Cu.

Zinc.

The patterns from the epitaxial growth of Zn on Cu (110) are shown in Figs. 48a and 48b. It is seen from Fig.48a that two perpendicular sets of parallel spot rows are present, in which the spot separations correspond to the c* and a* of the hexagonal zinc. The 205 diffraction appears in the plane of incidence whereas the 103 diffraction spot is not quite in the plane of incidence in Fig.48a. Hence the orientation of

Zn is (205), though in similar conditions Cd has (103) orientation.

The pseudo cubic structure of zinc is seen in the [001] azimuth (Fig.48b). The sharp and elongated spots show that the Zn crystals were atomically smooth. The appearance of a strong 103 diffraction spot in this azimuth is probably due to the fact that the centre of the zero order Laue zones is slightly above the central spot and hence diffraction due to (103) plane also appears.

The lattice constant of the zinc was calculated from Fig.48b, using the spacings of [110] rows of Cu as reference. "a" for zinc was found to be 2.642 A. The value for "a" by X-rays is 2.6595 A. (Wyckoff, 1948). From Fig.48a the value of "c" was found to be 4.180 A. The X-ray value for "c" of zinc is 4.937 A.

The c axis of the zinc was thus abnormally compressed by 15.3% during the epitaxial growth, though the a axis was effectively of normal length.

When Zn was deposited epitaxially on the Cu (100) face Figs. 49a and 49b were obtained. The 101 and 202 diffraction spots appear in the plane of incidence in both azimuths. The (101) plane of zinc is therefore parallel to (100) of Cu, with [100] of Zn along the cube face diagonal of the copper.

Table 11.

Intensity	Radius in cm	d in A.	hkl	Theoretical value in A.
f	0.580	4.20	200	4.24
f	0.618	3.94	011	3.96
s	0.699	3.48	210	3.48
s	0.738	3.29	201	3.27
s	0.839	2.90	120	2.89
f	0.915	2.66	021	2.64
f	1.085	2.24	202	2.21
vvf	1.125	2.16	400	2.12
f	1.174	2.07	320	2.08
f	1.301	1.87	031	1.90
s	1.400	1.74	420	1.74
vf	1.485	1.64	402	1.64
vf	1.618	1.51	040	1.54

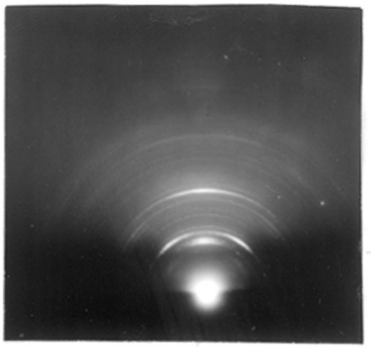

Fig 53

Lead carbonate

Lead.

Attempts were also made to deposit two-degree orientated Pb on Cu (110) face from alkaline and acid baths. But in both cases, instead of metallic Pb, a random or one-degree orientated Pb-compound was obtained. The compound was identified as lead carbonate. The pattern obtained from a one-degree orientated lead carbonate which was formed during deposition in the alkaline bath for 2 mins. at 5 ma./sq.cm. is shown in Fig. 53. The measurement of ring dimensions and spacings are shown in Table 11.

The lattice constants of rhombic lead carbonate are (Wyckoff, 1948) a = 8.468 A., b = 6.146 A., c = 5.166 A. Thus it is seen that the one-degree orientated $PbCO_3$ formed had practically the normal lattice dimensions.

4. Discussion.

From the above results it is seen that metals and compounds of different classes, such as body-centred-cubic Fe and hexagonal Cd, Zn and $Cd(OH)_2$ grow epitaxially on electro-polished Cu (110) and Cu (100) faces. With increasing time of deposition the deposits tend to be more and more di-orientated.

Cd retains its normal lattice dimensions on Cu (110), whereas the c axis of Zn is compressed by about 15%, although a retained its normal value, similar to the pseudomorphic ZnO

formed at room temperature on Zn, first observed by Finch and Quarrell (1933-34). Though Zn and Cd both belong to close packed hexagonal system their orientations on Cu (110) and Cu (100) are quite different. The orientations taken by Cd on Cu single crystal substrates are the same as those of ZnO on ZnS. Aminoff and Broome (1936) and Yamaguti (1935) observed (103) orientation of ZnO on (110) ZnS. The ~~last~~ first authors (1938) also observed (203) orientation of ZnO on (001) ZnS. Siefert (1940) has discussed the orientation of ZnO on (110) and (100) ZnS from the point of view of the ionic fitting across the junction region.

The rotational slip of ZnO on (110) ZnS in the planes $\{11\bar{2}0\}$ observed by Evans and Wilman (1950) has also its close analogy in the behaviour of Cd on Cu (110).

Zn neither behaves in the same way as regards orientations on Cu single crystals, nor shows any rotational slip tendency at all. This different behaviour of the two metals and the large compressibility of the c axis of Zn must be accounted for by the close similarity of the Zn atom radius to that of Cu, and the much larger radius of the Cd atoms.

Possibly Zn forms an alloy with copper, such as ϵ brass, having a composition varying between 80-86% Zn (by atomic proportion) at room temperature. Such alloys are also of the close-packed hexagonal types, like Zn, and have the following lattice parameters (Strukturbericht, 1937):

80% Zn (atomic proportion) a = 2.74; c = 4.294 (c/a=1.56)

86% Zn (atomic proportion) a = 2.76; c = 4.286 (c/a=1.55)

These dimensional values agree approximately with the experimental results

a = 2.64 A., c = 4.18 A and c/a = 1.58.

B. Influence of Alternating Current superimposed on Direct Current in Cathodic Crystal Growth.

1. Introduction.

Many workers have investigated the structures of cathodic crystals by optical microscopy, X-rays and electron diffraction. Finch and his collaborators (1936, 1937, 1947) distinguished three different stages in cathodic crystal growth process. During the first stage of deposition, the crystal growth and orientation are strongly influenced by the substrate The second is a transition stage in which the bath conditions begin to affect the orientation at the expense of the substrate influence. In the final stage, the deposit assumes a crystal

habit and orientation governed wholly by the bath conditions. This third stage is reached only in thicker deposits (but far more quickly with polycrystalline as compared with single crystal substrates). The orientations developed at the final stage have been explained by the above investigators from consideration of ionic mobility, by hydrogen codeposition and fault and crystal boundary effects. They pointed out that adsorption of hydrogen ions or atoms is a very important factor in determining the orientation.

The cathodic deposits so far investigated were obtained by a steady direct current. The influence of superposing an alternating current over a direct current in the cathode deposition process has not been studied in its effect on the crystal habit and orientation, though Kohlschütter and Schödl (1922) investigated the bahviour of dissolution and deposition potential of nickel as influenced by the superposition of A.C. on D.C.

By superposing A.C. on D.C. both the potential and the current become undulating, but always of positive value if the A.C. amplitude is suitable ~~in~~ (magnitude) and the varies with phase. This undulating potential and current might affect the crystal growth and orientation of the deposit, both of which might behave in a way different from that of the steady potential and current on the deposit conditions. Moreover this

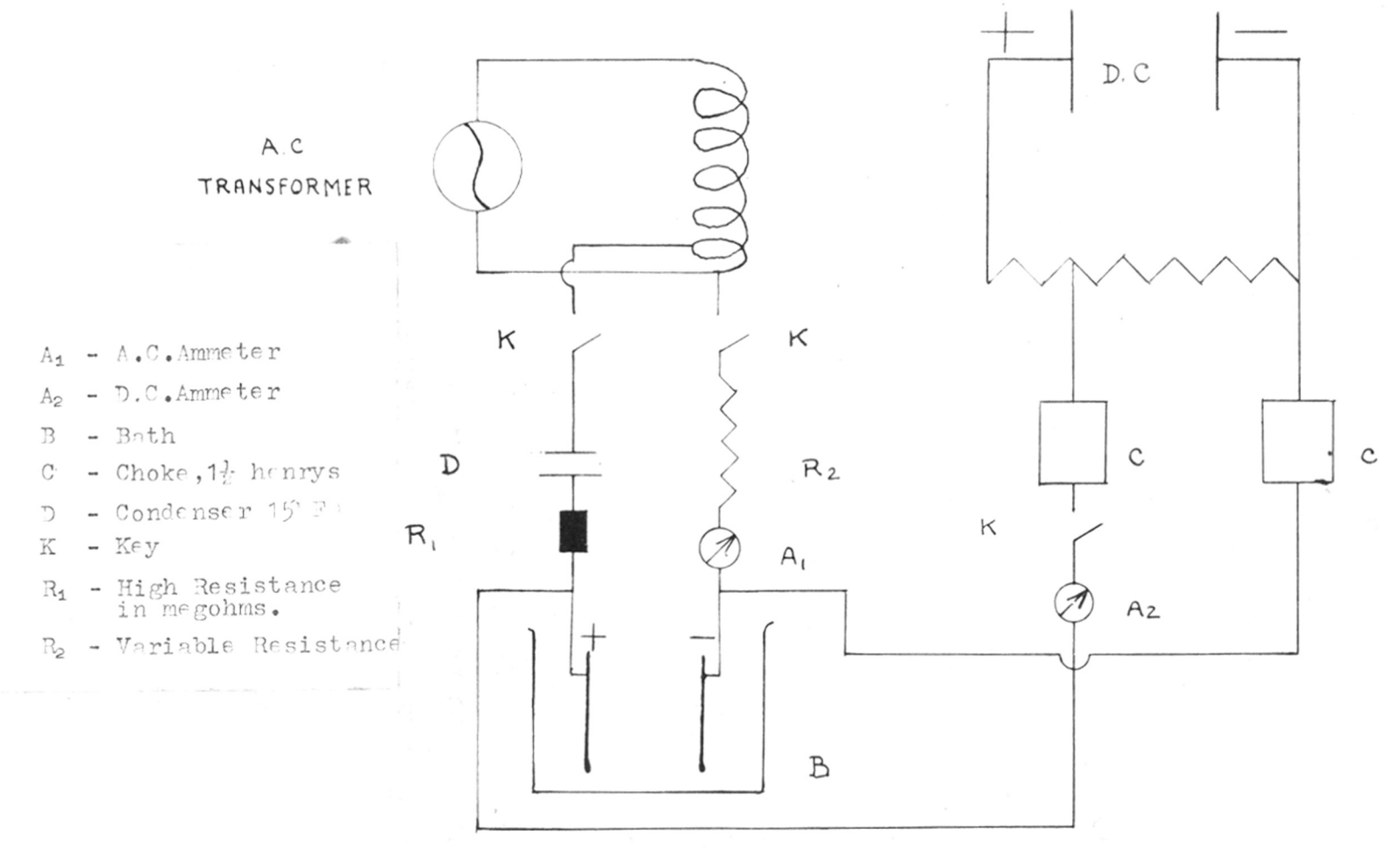
A.C
TRANSFORMER
A1 - A.C.Ammeter
A2 - D.C.Ammeter
B - Bath
C - Choke, 1½ henrys
D - Condenser 15
K - Key
R1 - High Resistance in megohms.
R2 - Variable Resistance
K
K
D
R2
R1
A1
D.C
C
C
K
A2
B

FIG. 54

undulating current might have some effect on the adsorption of hydrogen ions or atoms at the cathode surface, which has a strong influence on orientation, as was pointed out by Finch and his co-workers. Due to the variation in the intensity of potential and current, and the polarity (sometimes) of the cathode (which may revert to positive), the physical properties of the crystal may well be different from that of normal deposits. Hence a study of the deposits, especially their orientation, may throw some light on these properties. With these ideas in view, a preliminary investigation was carried out as described below.

2. Experimental.

The A.C. and D.C. systems are shown diagrammatically in Fig. 54. The main A.C. line was connected to the electrode through a series of condensers, variable resistances, a key and an A.C. ammeter. These condensers were of sufficient capacity to prevent D.C. from short-circuiting through the A.C. system. The D.C. voltage used was tapped from the main through a suitable resistance. The two leads were then connected to the two electrodes through a series of chokes, keys, a variable resistance and a D.C. milliammeter. The chokes were of sufficient value to prevent any short circuiting of A.C. through the D.C. system. During the deposition of any metal

D.C. 12.7 mA/cm²
A.C. nil

Fig 54a

GA 810

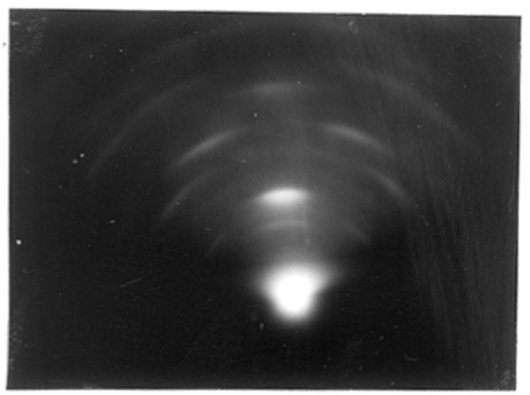

D.C. 12.7 mA/cm²
A.C. 14.2 " "

Fig 54b

GA 81

Nickel on copper, with or without
A.C. or D.C.

the same precautions were taken as were described in Section II, A.2). Polycrystalline copper was used as the specimen. The method of preparation of its surface is already described in Section I. The specimen was dipped first and then both the A.C. and D.C. lines were switched on. The A.C. used in the main was of 50 cycle frequency. The composition of the baths used for deposition have already been shown in Section II, A.

3. Results.

The effects of superposing A.C. on D.C. in crystal orientation at different temperatures were investigated in the cases of iron and nickel deposits. A rather detailed study of crystal orientation at different current density was made with nickel deposits. The results are shown in Tables 12 and 13.

It is seen from Table 12 that, though the orientation of nickel varies from weak (111) to medium (110) and strong (210) with different current densities, at room temperature, there is no change in orientation caused by superposing A.C. on D.C. At high temperature of deposition, though the orientations changed from those at room temperature, no influence was observed by superposing A.C. on D.C. In the iron deposit, also, A.C. had no effects on crystal orientations, either at low or high temperature (see Table 13).

Table 12.

Nickel bath composition - $NiSO_4.7H_2O$ 240 g./l;
H_3BO_3 30 g./l.

Expt.	Direct Current c.d. in ma/sq.cm	Alternating Current c.d. in ma./sq.cm.	Temp °C.	Time in mins.	Orientation.	Fig
1	3.0		27	40	weak (111)	
	3.0	4.8	27	40	weak (111)	
2	6.4		27	20	medium (111)	
	6.4	8	27	20	weak (111)	
3	12.7		27	40	weak (110) strong (210)	
	12.7	14.2	27	40	medium (110) strong (210)	
4	12.7		75	30	strong (100) medium (10$\bar{1}$0)	54a
	12.7	14.2	75	30	strong (100) medium (10$\bar{1}$0)	54b

Table 13.

Iron bath composition $FeSO_4(NH_4)_2SO_4.7H_2O$ 350 g./l.
H_2SO_4 2.5 g./l.

1	12.7		27	20	medium (100) strong (111)
	12.7	14.2	27	20	medium (100) strong (111)
2	12.7		75	20	strong (110)
	12.7	14.2	75	20	strong (110)

4. Discussion.

In a very thick deposit, the orientation developed depends on the bath conditions, i.e. temperature, current density, etc. The effect of superposing A.C. on D.C. is that in one phase, the magntidue of the D.C. component is augmented by the A.C. component and in the next phase it is decreased by the same amount, and if the A.C. component is larger than the D.C., the polarity of the specimen will change with the phase.

With this picture in mind, the experimental results can be explained easily. In the above experiments, the magnitude of the A.C. was slightly higher than that of the D.C., hence the polarity of the cathode changed to positive, for a small part of the time. As a result, the deposition occurred with variable magnitude of current during one half cycle and in the next half cycle the deposit must partly have gone into solution (with change of polarity), then again deposition occurred and so on. It seems from the results that polarity changes do not affect the orientation of the deposit, but only lead to dissolution of part of the crystals. Thus the orientation is solely determined by the bath conditions, i.e. mobility of ions, current density, concentration, etc. As practically no other change is caused in bath conditions, except slight variation of current density, due to superposition of A.C. on D.C., it seems natural that the orientation should remain the same. The only

other change that may possibly be caused is the modification of physical properties, i.e. shape, stress and strain in the crystal, hardness, etc. It is quite likely that stress in electrodeposits may be modified to some extent by this way, but this has not yet been tested. Nor has the effect on adhesion been investigated.

C. Cathodic Crystal Growth in a Magnetic Field.

1. Introduction:-

Crystal growth in a magnetic field has been studied by some workers, but without much positive result. Bergala and Gorski (1934) observed that the rates of crystallisation of water, salol and diphenylamine are not affected by fields up to 15,000 gauss. Steacie and Stevens (1934) found that the rate of crystallisation of sodium thiosulphate was not affected whereas in the case of nickel sulphate there was a slight increase in the rate of growth which, however, was not much greater than the experimental errors.

Atma (1938) found that Bi powder was orientated with its principal crystal axis in the direction of the field if allowed to fall freely in the magnetic field. He also observed that crystals of bismuth can grow from cooled liquid bismuth in the direction of the field, when the nucleus of the crystallisation was able, after formation, to rotate freely in the field. Blandin (1949) studied the crystal growth of various salts from concentrated solutions in a magnetic field of 15,000 gauss with a polarising microscope. He observed that sulphates of Mg, Zn and Ni crystals align themselves in a direction perpendicular to the field. He also observed that in the formation of copper sulphate crystals the axis of more magnetic permeability was along the direction of the lines of

force. The double sulphates of ammonium and magnesium, and potassium and iron, align themselves in different directions in the magnetic field.

Bozorth (1925) did not find any change in the orientation of electrodeposited nickel in a magnetic field, but he did not state the strength of the field.

Yang (1948), working in this laboratory, has observed that electrodeposited Fe, Ni and Co on a polycrystalline polished brass, do not change their usual orientations even when deposited in a magnetic field of 5400 gauss strength. He also observed a tendency of outgrowing habit of the Fe deposit in the magnetic field when the substrate was iron.

The present work was intended to investigate the effect of a magnetic field on the orientation and habits of Fe deposits on Fe single crystals as well as polycrystalline brass substrates. Some experiments were also carried out to see if the habit of electrodeposited iron in a magnetic field is analogous to the powder patterns or Bitter figures (Bitter, 1931) formed on ferromagnetic substrates, when a colloidal magnetite is allowed to settle on a ferromagnetic material under a weak magnetic field.

Bitter figures of various ferromagnetic materials have been studied by many workers (Bitter, 1932; Elmore, 1937; Williams, Bozorth and Shockley, 1949; Bates and Heale, 1949;

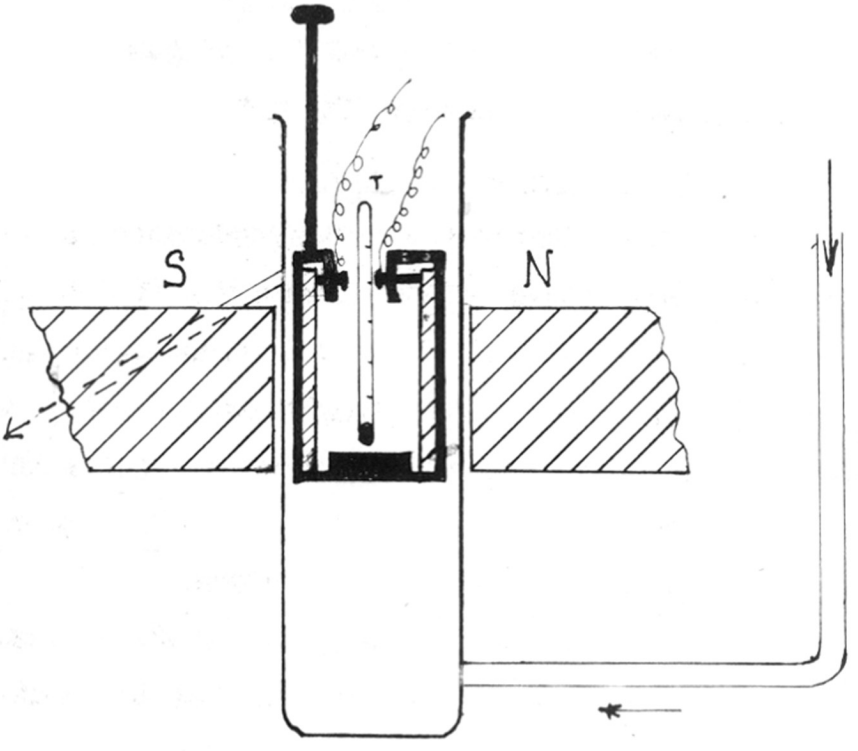

Fig 55-

and others). The formation of these Bitter figures is due to the presence of magnetic domains in a ferromagnetic material (Heel, 1944; Brown, 1945).

2. Experimental.

The technique of deposition of iron is similar to those already described in Section II, A.2.

Electropolishing of Iron.

Fe (100) faces were electropolished in a solution containing 765 cc. of acetic anhydride, 185 cc. perchloric acid (S.G. 1.61) and 50 cc. water. The temperature was kept below 25°C. The c.d. used was 8 amp./sq.dm. The cathode was a rectangular piece of soft iron about 10 sq.cm. in area and was at a distance of 3 cm. from the anode. The anode and cathode were kept vertically facing each other.

After electropolishing, the specimens were dipped in 1% picric acid solution in ethyl alcohol to remove the oxide (if any) formed during electropolishing.

The deposition of iron was carried out in a test tube of about 3.5 cm. diameter, placed within the pole gap of a permanent horseshoe magnet. The anode and cathode were rigidly fixed in a bakelite frame which could be moved freely inside the test tube. A slow constant flow of electrolyte solution was maintained by the inlet and outlet tube attached to the test tube so as to avoid changes of concentration. Screws used in the frame were made of brass. The frame was

mag
X24

Fig 56

Bitter figure pattern of
ferrosilicon alloy

then coated with a collodion film to prevent contamination with the electrolyte. The magnet used was of 4,000 – 5400 gauss strength.

Preparation of Colloidal Magnetite.

1 gram of ferrous chloride and 2.7 grams of ferric chloride were dissolved in 150 cc. of water and 2.5 grams of NaOH in 25 cc. of water were added to it with stirring. The precipitate was allowed to settle and was washed thoroughly with distilled water and finally rinsed with 0.01 N HCl. The precipitate was then mixed with 500 cc. soap solution (0.5% concentration) and boiled. Before use the colloidal magnetite was always boiled & cooled to room temperature.

Technique of forming Bitter figure patterns.

A drop or two of colloidal magnetite was placed on the electropolished specimens kept in a weak magnetic field and a thin glass slide was placed on the liquid. The pattern formed on the surface was then examined under a low power microscope and microphotographs were taken.

The specimens were always demagnetised by placing in an alternating field and decreasing the current gradually to zero, before any further experiment was made.

A typical Bitter figure pattern formed on a ferro silicon alloy (about 2.5% Si) single crystal is shown in Fig.56

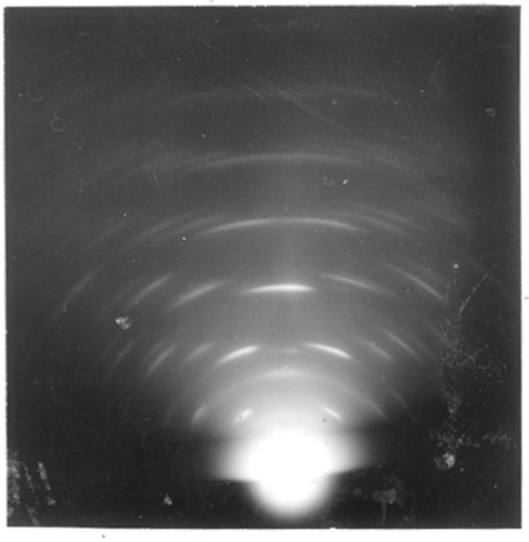

Fig 54 a

Fe deposited in magnetic field

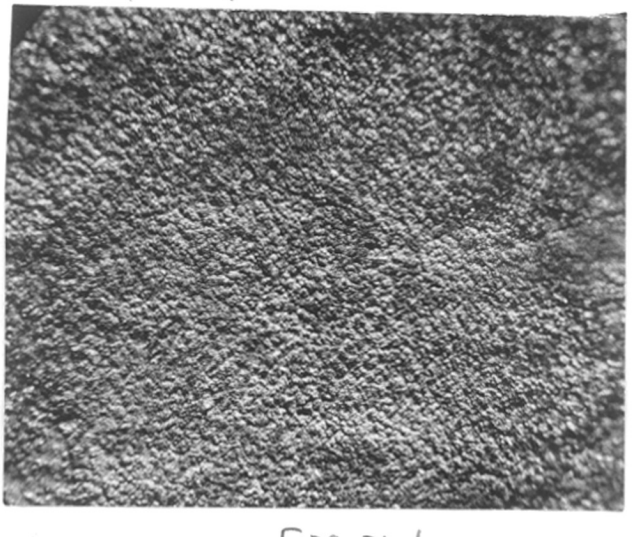

mag

X43

Fig 54b

Fe deposit on Fe (100) with field
⊥ the Cathode

mag x43

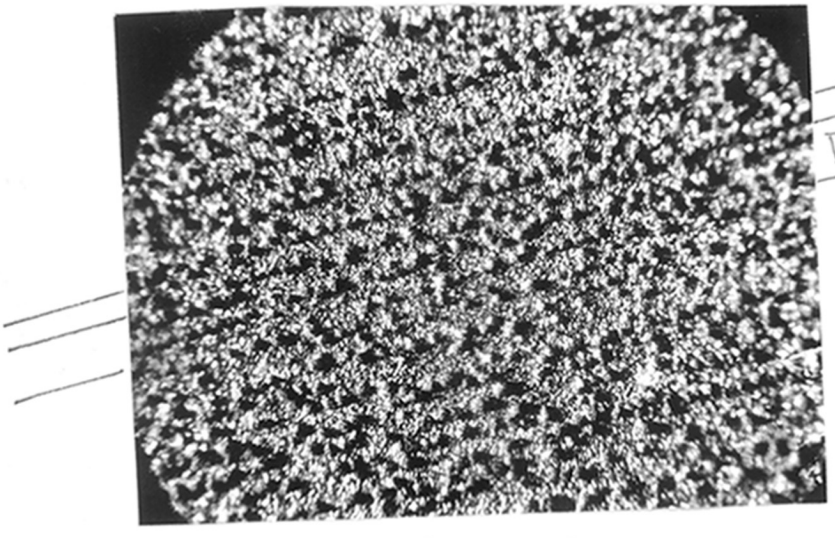

Fig 58

Fe deposited of Fe (100) with field
⊥ the surface

3. Results.

The results of the deposition of Fe on the Fe (100) surface are shown in Table 14.

Table 14. c.d = 37.5 mA/cm²

Expt.	Substrate	Temp °C	Time min.	Field	Orientation	Fig.
1	Fe (100)	20	60	—	(111)	
2	Fe (100)	20	60	⊥	(111) ···	57a, 57b
3	Fe (100)	20	60	∥	(111)	
4	Fe (100)	80	10	⊥	Continuous growth and random.	
5	Fe (100)	80	60	⊥	No pattern	58
6	Fe (100)	80	60	∥	No pattern	

It is seen that the orientation of the deposit crystals was not affected by the magnetic field at all, though the deposits formed in the magnetic field were comparatively rough.

The orientation and microphotographs of the deposit crystals in experiment 2 are shown in Figs. 57a and 57b. Fig.57b shows that the deposit crystals had a tendency to grow along the [010] axis of the Fe (100) surface. Similar results were also obtained in experiment 3, though the rows of crystals were not so prominent. Fig.58, in experiment 5, shows the rows of crystals aligned along the [011] direction of the Fe (100) surface.

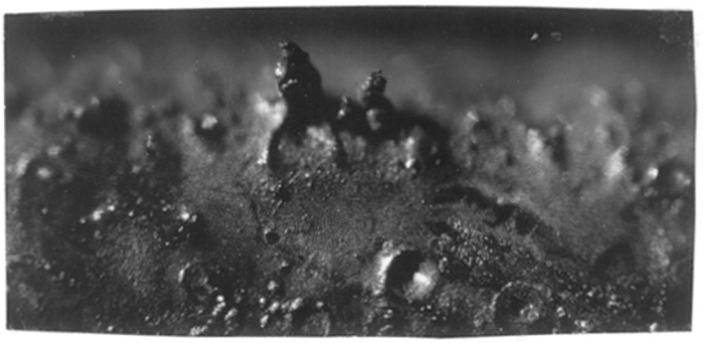

mag
X43

Fig 59

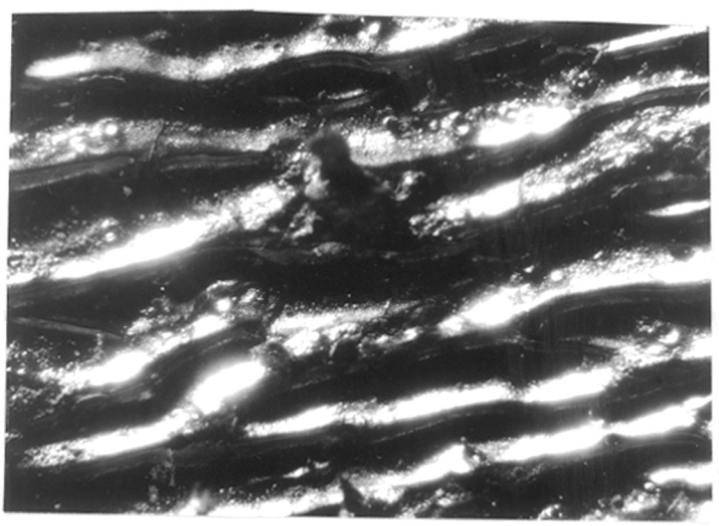

mag
X24

Fig 60

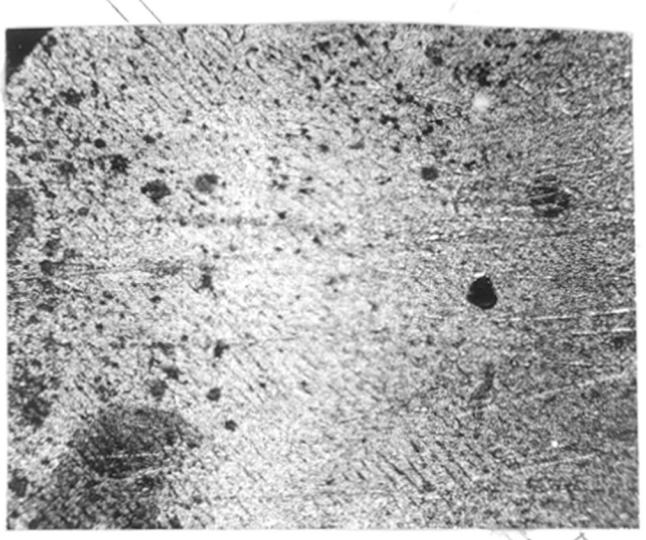

mag X110

[010] Fe

Fig 61

Bitter trigure pattern of Fe(100)

When Fe was deposited on a ~~brass~~ iron cathode, in a field (5400 gau inclined at about 45° to the cathode, it was observed that the deposit crystals had a tendency to grow outwards along the direction of the magnetic field (Fig.59). When the field was normal to the surface the crystals also formed long outgrowths in the direction of the field. Fig.60 shows strong outgrowth of the Fe deposit in the form of ridges on brass with the field normal to the surface It was also further observed that on the part of the deposit nearest to the pole of the magnet, the outgrowth tendency was much greater than at any other place further away from the pole.

A Bitter figure pattern formed on the Fe (100) surface is shown in Fig.61. The pattern consists of parallel lines along the [010] axis. The pattern was similar, whether there was a magnetic field present or not, or whether the direction of the field was along the axis or in any other direction.

4. Discussion.

It is seen from the above results that the habit of the Fe deposits is greatly influenced by the field. The crystals have a tendency to grow along the lines of force, forming long outgrowths when the field is strong.

On iron single crystal substrates, the tendency of the deposit crystals to grow along [010] and [011] is rather analogous to the formation of Bitter figures. On the Fe (100) face the lines in the Bitter figures are generally along [010]

though in a strong field they may also be along [011]. The Bitter figure pattern is generally influenced by the magnetic anisotropy of the substrate. In the case of the Fe single crystal, the direction of easy magnetisation is mainly along [100] (Bates, 1948).

The colloidal magnetite particles are attracted along this axis and settle there, and hence the pattern formed consists of rows of lines parallel to [010) axis on Fe (100).

When iron was deposited in the field normal to the cathode surface due to the strong magnetic anisotropy of the Fe crystals along the [010] axis of Fe (100), the magnetic vector is the strongest along [010]. As a result, the Fe ions, which are themselves paramagnetic will be more attracted along this [010] axis and deposited there. This will help further outgrowth of the deposit crystals and the crystals grow along this direction of easy magnetisation.

Fe crystals have also [011] as a direction of easy magnetisation. Hence, under certain conditions, the Fe deposit may grow along that direction, as has been found in Fig. 58.

Thus the form of the Fe deposit in the magnetic field is analogous to the Bitter figure pattern, obtained on the same substrate, in the case where there is a crystal having strong magnetic anisotropy.

Section III.

Crystal Growth in Chemical Displacement of Metals.

1. Introduction.

The deposition of a metal by the chemical displacement of another is a process much used in the metal-finishing industr For example, iron can be coated with copper, nickel, silver or gold, simply by immersing in suitable salt solutions of these metals.

Depoits obtained in this way often vary considerably in physical properties, i.e. crystal habit, adhesion, reflectivity, etc. from those obtained by the corresponding electrodeposition processes. Thus if copper is deposited on iron or zinc by chemical displacement a spongy non-adherent coating is usually produced (Blum and Hogaboom, 1930). Nickel deposited on zinc in this way is usually black and non-adherent. Silver deposited by immersion on most of the metals is also generally non-adherent. Since the deposition of precious metals like silver, gold or platinum by displacement is of considerable technical importance, the process is controlled in such a way that an adherent deposit is obtained.

This displacement process has its special applications in many fields.

The study of crystal growth in chemical displacement process is of great importance, because the physical properties of a metal depend largely on its mode of growth. In order that a metal may be used as a coating on another, either for protection against corrosion or for decorative purposes, its adhesion to the substrate, its mode of growth, habit and also appearance are of importance. A study of crystal growth in the displacement process is therefore desirable. Another aspect of the problem is how far the process of crystal growth may be compared with other processes, like growth from the vapour state, solution or melt, or from the ionic state by the process of neutralising the charge (electrodeposition).

Comparatively few results on the structure of metal deposits formed by displacement are yet available. Tsuboi (1928) investigated by X-rays the spongy deposit of silver, obtained by immersing a polycrystalline copper wire in $AgNO_3$ solution. He found that in the silver deposit the micro crystals had (111) orientation. He (1929) also obtained (~~1930~~) (111) orientation for Pb and (0001) for Cd on zinc by displacement.

Finch and Sun (1936) investigated by electron diffraction the structure of platinum deposits obtained by the displacement of polycrystalline copper and silver. They found

that the lattice constant of the deposited metal did not correspond to the pure platinum or pure copper, and concluded that an alloy of platinum, possibly $PtCu_3$, was formed.

An extension of the work of Finch and Sun has been made in the following researches. Since adhesion of a metal to another depends much on whether the crystal growth is epitaxial or otherwise, the growth on single-crystal substrates has been studied.

2. Experimental.

In these investigations the substrates used were (110) and (100) faces of copper single crystals, a single crystal of ferro-silicon alloy (about 2.8% Si), a polycrystalline mild steel surface, and a thin film of electrodeposited iron. The methods of preparation of the (110) and (100) faces of copper single crystals were described in Section I and those for iron and ferro-silicon alloy in Section II.

The iron film was prepared in the following way:-

Copper was deposited on a polished stainless steel disc at a current density of 0.2 amp./sq.dm. for 30 minutes, using ~~iron~~ copper as an anode, from the copper cyanide bath referred to in Section II A. The stainless steel disc, coated with copper, was then taken out from the solution, washed thoroughly and then immersed in the iron bath as cathode. The composition

of this bath has already been stated in Section II, A. Iron was deposited at a current density of 1-3 amp/sq.dm. for 15-20 seconds, using an iron anode. The cathode was then washed thoroughly in distilled water. The composite coating of iron and copper was stripped from the stainless steel by a knife and the coating was kept immersed in 40% KCN solution until all the copper had dissolved. The thin iron film was lifted out on a nickel gauze and washed thoroughly by floating on several changes of water. The film was then treated as below:

a. For deposition of copper: N/10 solution of copper sulphate.

b. For deposition of silver: AgCN - 3.5 g./l
KCN - 3.7 g./l.
K_2CO_3 - 3.8 g./l

After displacement, the specimens were washed, wetted with propyl alcohol, and quickly transferred to the electron diffraction camera.

In order to measure the lattice constants of the deposited metals, either graphite powder or 'Aquadag' was used. Comparing with $d_{11\bar{2}0}$ = 1.228 kx = 1.230 A. for graphite, the λL was calculated and the lattice constants found.

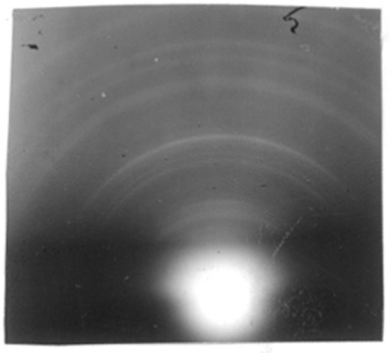

Fig 62

GW77

Cu, with graphite

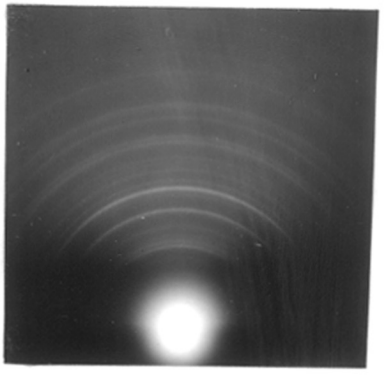

Fig 63

GW170477

Cu_2O with graphite

3. Results.

The results obtained by various treatments are described below.

By treating the ferro-silicon single crystal in N/10 solution of copper sulphate for 20 secs., a copper deposit was obtained which yielded Fig.62. The ring dimensions and the lattice constant found experimentally are shown in Table 15.

Thus the lattice dimensions of the deposit corresponds to that of copper within the experimental error.

The copper deposit obtained by treating mild steel had the lattice dimensions shown in Table 16. (Fig.63).

The lattice constant, 4.292 A., corresponds to Cu_2O. The X-ray value = 4.252 A.

The measurements of the pattern obtained by treating an electrodeposited iron film in copper sulphate solution are shown in Table 17. Fig.64 shows the pattern.

The lattice constant found = 2.861 A. which corresponds to Fe, the lattice constant of which is 2.860 A. (Wyckoff, 1948)

Table 15.

Intensity	R in cm.	d in A.	hkl	a in A.
f(d)	1.160	2.095	111	3.629
f	1.326	1.833	200	3.666
m	1.878	1.294	220	3.661
* f	1.976	1.230		
m	2.198	1.106	311	3.665
vf	2.301	1.054	222	3.659
vf	2.676	0.9082	400	3.633
f	2.891	0.8408	422	3.760 ≠
f	2.983	0.6934	333	3.602

* graphite ring 1120

≠ result too high and hence neglected.

m = medium; f = faint; v.f. = very faint. d = diffuse

Average value a for Cu found = 3.641 A.

a for Cu (Wyckoff, 1948) = 3.608 A.

Table 16.

Intensity	R in cm.	d in A.	hkl	a in A.	
vf	0.790	3.175	110	4.48	✗
vf	0.999	2.509	111	4.346	
f	1.158	2.165	200	4.330	
* f	1.230	2.038			
vf	1.324	1.893	210	4.234	
f	1.425	1.760	211	4.315	
m	1.647	1.524	220	4.308	
vf	1.853	1.326	310	4.197	
m	1.936	1.295	311	4.295	
* f	2.038	1.230			
f	2.333	1.074	400	4.296	
f	2.547	0.9841	330	4.275	
f	2.625	0.9500	420	4.291	

* graphite ring.

✗ value too high and hence neglected.

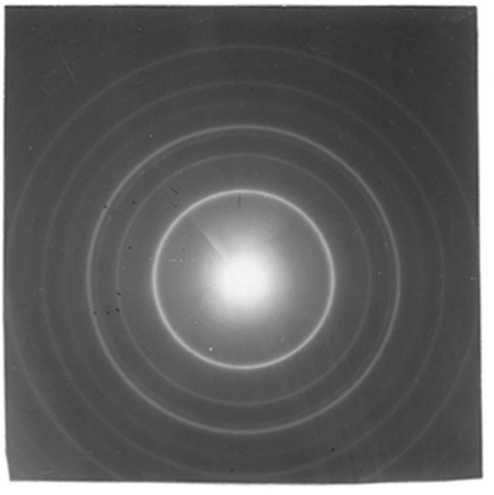

Fig 64

G4109

Iron

Table 17.

Intensity	R in cm.	d in A.	hkl	a in A.
vs	1.241	2.030	110	2.860
m	1.762	1.430	200	2.860
* s	2.048	1.230		
s	2.158	1.167	211	2.856
f	2.484	1.014	220	2.863
m	2.778	0.9066	310	2.865
f	3.038	0.8291	222	2.870
m	3.289	0.7657	321	2.856

* graphite ring ($11\bar{2}0$)

A similar determination of the lattice constants of silver obtained by displacement at a copper single crystal surface was made and the results are shown in Table 18 along with those of the other metals.

Table 18.

Substrate	Deposit	a_0 (found) in A.	a_0 (Wyckoff) in A.
Ferrosilicon single crystal	Cu	3.641	3.608
Polycrystalline iron.	Cu_2O	4.292	4.252
Cu (100)	Ag	4.082	4.077
Cu (110)	Ag	4.041	4.077

Ag on Cu (110)

B

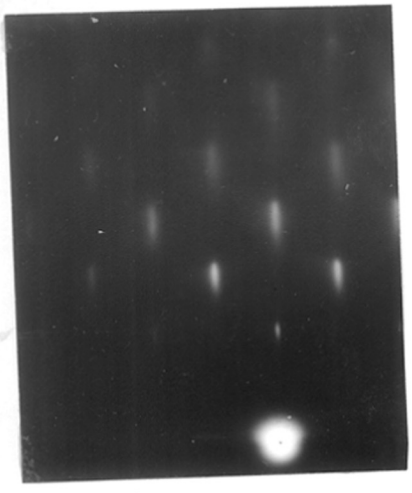

Fig 65 a

Beam along [001]

GW 1187

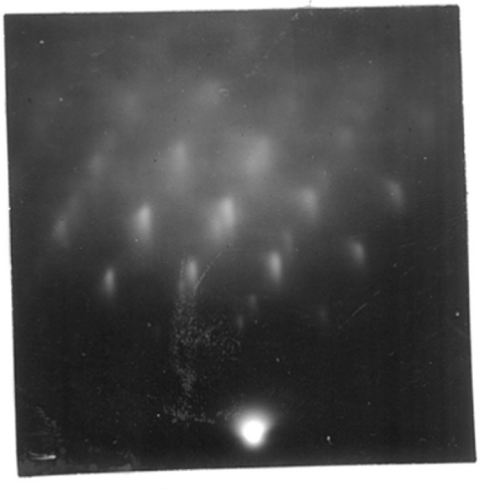

Fig 65 b

Beam along [1 1 0]

GW 1182

Ag on Cu (100)

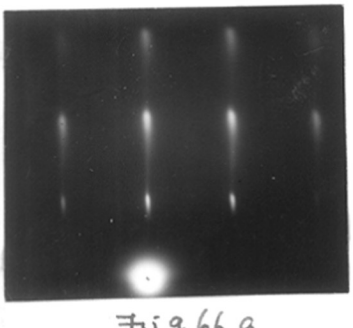

GW 1074

Fig 66 a

Beam along [001]

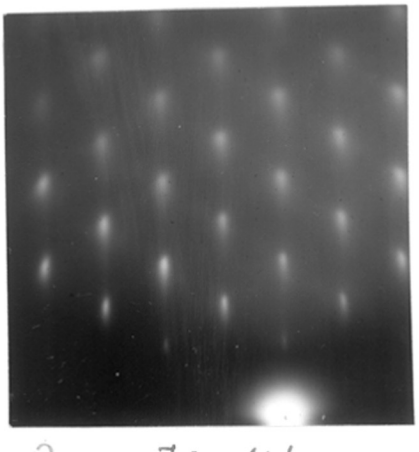

GW 1072

Fig 66 b

Beam [0 1 1]

Silver by displacement

The observed orientations of Ag growing on Cu (110) and Cu (100) faces are shown in Table 19.

Table 19.

Substrate	Deposit	Orientation	Fig.
Cu(110)	Ag	(110) Ag // (110) Cu [001] Ag // [001] Cu	65a 65b
		Sometimes with twinning on {111} planes.	
Cu(100)	Ag	(100) Ag // (100) Cu [001] Ag // [001] Cu	66a 66b
		Sometimes with twinning on {111} planes.	

The sharp and elongated diffracted spots due to silver (Figs. 65a and 65b) show that the deposited crystals were atomically smooth and well defined. The extra spots occurring (Fig.65b) are due to twinning of Ag on {111} planes.

An interesting pattern of Ag on Cu (110) is shown in Fig.67. Here, in addition to the normal spots and those due to twinning of Ag, two series of faint straight lines appear which pass through the twinspots. This indicates that the beam was refracted by some well-defined facets on the Ag formed by the displacement process. From a consideration of the straight lines, the facets are found to be {111}. A similar pattern of nickel on a Cu (110) face was obtained by

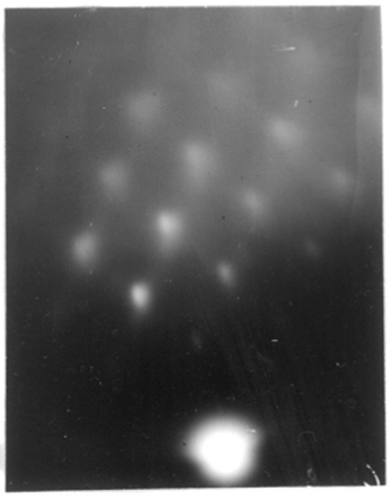

Fig 67

GU 1185

Ag lay dis placement. showing
{111} facets

Beam along
[011]

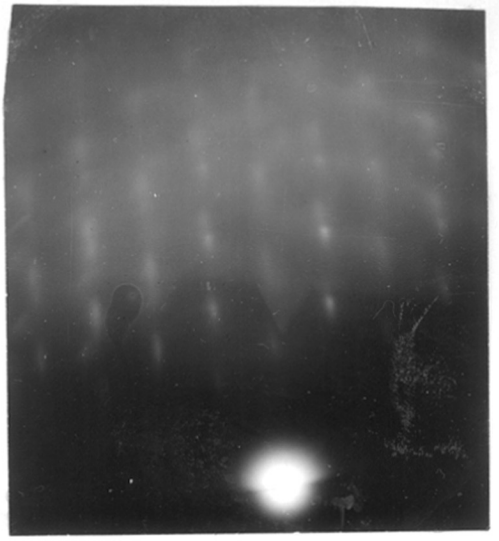

Fig 68a

Beam along
[001]

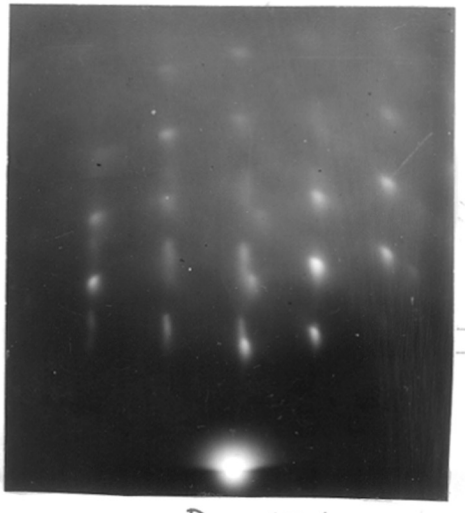

Fig 68b

Ag key displacement
on Cu(110) face

Cochrane (1936) by electrodeposition. The orientation of the Ag developed on Cu (110) was always with a cube edge of Ag parallel to the cube edge of the Cu, and usually accompanied by twinning on {111} planes.

On the Cu (100) face Ag developed (100) orientation the cube edge of the silver deposit being along the cube edge of Cu (Figs. 66a and 66b), sometimes along with twinning. An interesting case of the development of a new orientation in addition to the parallel growth on the Cu (100) faces is shown in Figs. 68a and 68b. In addition to the elongated diffraction spots due to the parallel orientation of Ag, there are sharp spots of rectangualr pattern, which suggest that the (111) plane of Ag was parallel to the Cu (100) face. Further it is seen that these diffracted spots do not pass through the central spot, but are shifted sideways to a position of the next higher order. This suggests that the plane (111) is nearly parallel to the surface but is tilted by about 10°. This is again confirmed from the diffraction pattern when the beam was along [001] azimuth (Fig.68b). The diffracted spots due to parallel growth also are visible. The 222 diffraction spot is not exactly in the plane of incidence. The curving of the Laue zones also show that the centre of these diffraction spots are about 10-12° away and slightly below the shadow edge. The orientation thus appears to be not quite (111), parallel to

Ag on Cu(100)

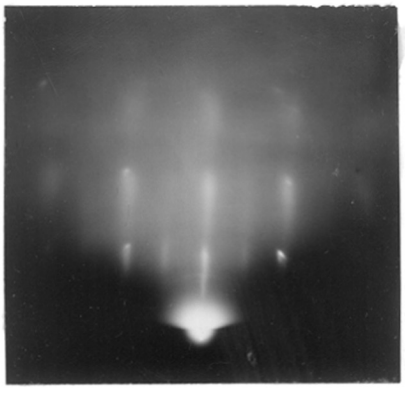

Beam along [001]

Fig 69

Cu 1075

Silver, twinning planes {332}

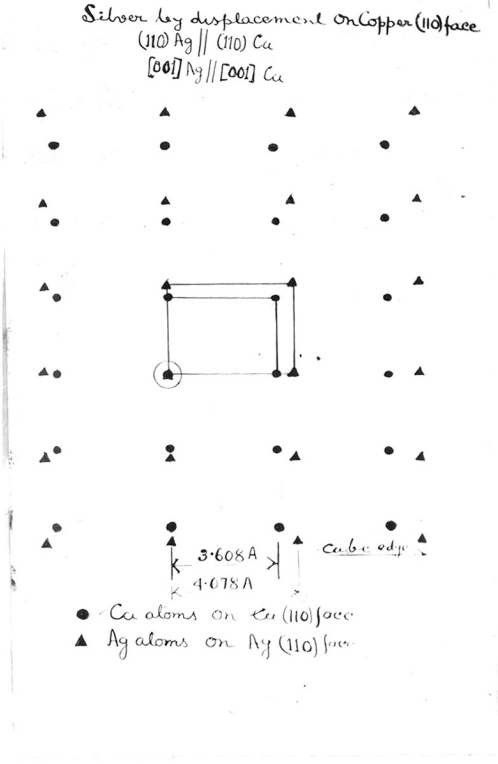

Fig 70

Atomic fitting of silver on Cu (110) face.

the surface, but in between (111) a plane and (112), parallel to the surface. A similar sort of orientation was also observed in the case of Cu_2O formed on Cu (100) in water (~~hot and cold~~) or in cold alkaline solution (see Section I).

Silver also showed twinning on planes other than {111}. Fig.69 shows such a pattern. In addition to the normal silver spots, there are some strong spots due to the formation of twinned crystals. The pattern is similar to that obtained by Ellsman and Wilman (1948) when PbS twinned on {332} planes. This suggests that the twinning planes of silver, in this case were {332}.

The epitaxial growth of Ag on a Cu (110) face is shown in Fig.70. The lattice constants of Ag and Cu being 4.078 A. and 3.608 A. respectively, the percent contraction of Ag along the cube edge would be 13.00%.

Discussion.

Cu, Cu_2O and Fe :- Cu obtained by displacement on a ferrosilicon crystal retains its normal lattice structure. As copper oxidises relatively easily in air, a film of Cu obtained by the displacement process was oxidised to Cu_2O. The lattice constant of such Cu_2O is also normal.

Silver:- Silver obtained by displacement on Cu single crystals seems to retain its normal lattice constant value.

Silver grows with parallel orientation on Cu (110). On the Cu cube face it has not only parallel (100) orientation, but also appears to develop orientation in between (111) and (112) planes parallel to Cu (100).

It has been observed, Fig. 67, that during the parallel growth of Ag on Cu (110), {111} facets appear. The appearance of a refracted beam along a direction perpendicular to facets {111}, shows that the crystals are formed in such a way that two well defined facets of {111} type appear.

In the epitaxial crystal growth of Ag displacing Cu, the Ag atoms are deposited on the copper crystal layer by layer. Due to the difference in the lattice constants of Ag and Cu (about 13.0%), the atomic fitting will not be perfect. As a result of "misfit" of atoms, a stress will be generated near the Ag-Cu interface. As the film thickens, the stress will be more and more pronounced and finally may be relieved by a mechanical twinning process. The {111} and {332} twinning observed in epitaxial growth of Ag on Cu are probably of this type.

Consider the mechanism of the displacement of the metal. Every metal has a characteristic electrode potential, as referred to that of the hydrogen electrode. Hence the mechanism of chemical displacement is essentially that of electrodeposition. When a copper crystal is immersed in

silver solution, due to electrode potential difference. Silver cations are discharged and deposited on the copper substrate and copper ions go into solution. In this way deposition continues till the whole surface is covered by silver.

The deposition of silver by displacement process is analogous to the electrodeposition process, the only difference being that in this case, the current though feeble, is drawn from the galvanic cell itself. During the displacement process the solution is electrolysed by this feeble current and the metal is deposited over the exposed surface.

During this deposition process, the substrate material also goes into solution and if the concentration of substrate metal ion in solution is high or if other conditions are favourable it may be deposited again along with the other metal. Hence co-deposition in the form of alloy is quite possible on the bulk of the substrate surface.

It will be seen from the analogy of displacement to electrodeposition that the epitaxial growth is also an essential mechanism in this case of displacement of metals. It may be suggested that a further analogy is likely, in that if the metal could be deposited, by displacement, to a reasonable thickness, probably the deposit would be finally one degree orientated, i.e. all the crystals would have a

common plane parallel to the substrate otherwise randomly disposed in all azimuthal directions. An electron diffraction study of deposited metals by displacement on single crystal substrates from simple ion baths as well as complex baths at different thickness should throw light on this aspect and test the above hypotheses.

Summary.

From the electron diffraction study of the crystal growth in the different processes, i.e. anodic, cathodic, or displacement, it can be concluded that the crystal growth processes are fundamentally similar, though the mechanism of the deposition is different in each case.

During the first stage of the crystal growth, the deposit, in general, grows epitaxially either with the normal lattice structure or with a modified pseudomorphic form. Due to the misfit between atomic positions in the deposit and the substrate, a stress will be generated at the interface, and it may be relieved either by mechanical twinning or translational, or rotational slip or by recrystallisation.

With the increase of thickness of the deposit, the substrate influence becomes less and less and a stage is reached when the substrate influence is counterbalanced by other factors such as bath conditions. In this stage, the crystal growth tends towards a random disposition.

With further increase of thickness of the deposit, the influence of the bath conditions will prevail and a preferential growth will occur in those crystals which have a definite net plane parallel to the substrate. The orientation

thus developed depends upon the bath conditions.

In the case of the deposition by displacement the second and third stages of the process have not yet been tested.

In the thick deposit a magnetic field does not appear to affect the crystal orientation, though it may greatly modify the crystal habit, so that the growth occurs along some particular directions depending upon the magnetic anisotropy of the substrate and the direction of the field.

The superposition of A.C. on D.C. also did not cause any change in the orientation of Ni and Fe deposits on polycrystalline copper discs.

The other main results obtained are summarised below.

1. In the initial stage of anodic oxidation of Cu (110), a pseudomorphic cupric oxide was formed, with its b axis nearly double the b axis of the normal CuO. With increase of deposit thickness the CuO was formed with its normal structure. The orientation of CuO varied with the current density used.

2. With 15-20% NaOH solution mainly two-degree orientated Cu_2O was formed on Cu (110), having a parallel orientation. Twinning of Cu_2O on $\{111\}$ has been observed for the first time.

3. Anodic oxidation of Cu (110), Cu (100) and polycrystalline copper and brass gave rise to the same one-degree orientation of CuO under the same bath conditions. No sign of zinc or zinc oxide was observed in the case of brass at about 80°C.

4. Anodic ~~oxidation~~ treatment of Cu (110) in conc. HCl developed facets of {111} and {100} and the inner potential of the {111} Cu surface was measured. Anodic ~~oxidation~~ treatment in HCl also produced disorientation of a large proportion of the copper crystals.

5. By immersion in alkaline solution or water, Cu_2O grows with (110) parallel to Cu (110) surfaces and with (221) of Cu_2O parallel to Cu (100) surface. There is some evidence of the relief of epitaxial stress by rotational slip on the Cu_2O-Cu interface.

6. Epitaxial growth of Cu_2Br_2 on Cu (110) by anodic treatment yielded (111) orientation on Cu (110) and with greater thickness it became random.

7. One degree orientated CuO, when rubbed unidirectionally, was transformed to two-degree orientated CuO, with $(11\bar{1})$ plane parallel to the surface and [011] along the rubbing direction.

8. The epitaxial growth of Fe, Cd, Zn, $Cd(OH)_2$ on Cu single crystals was also studied. Fe grows with (211) and (110); Cd with (103) and (203) and Zn with (205) and (101) parallel to

Cu (110) and Cu (100) respectively. $Cd(OH)_2$ also developed (0001) orientation on Cu (110). Zn appears to have either a pseudomorphic structure or ~~develop~~ form an ϵ phase alloy with the copper. Cd, on the other hand, had its normal lattice dimensions, but showed a directed disorientation, which may be due to rotational slip on $\{11\bar{2}0\}$ planes.

9. Cu and Ag obtained by displacement process retained effectively their normal lattice dimensions. Ag deposited by displacement grows in parallel orientation on Cu (110) and Cu (100). Twinning on $\{111\}$ planes was observed and there is evidence in one specimen of twinning of Ag on $\{332\}$ planes.

Acknowledgements.

The author is indebted to Professor G.I.Finch, M.B.E., D.Sc., F.R.S., for his constant interest and valued advice during the progress of the work.

The author also wishes to thank Dr.H.Wilman for many helpful discussions.

Finally, the author wishes to record his thanks to the Calcutta University for awarding him the Radhika Mohon Scholarship, which enabled him to carry out his research.

References.

Aminoff and Broome, Nature, 137, 995, 1936.

Aminoff and Broome, Kungl.Svenska.Vet.Hand., 1938, 1b.

Arms, Ann.Physik, 1938, 32, 489.

Bates, Modern Magnetism, 1948

Bates and Neale, Physica, 1949, 15, 220.

Bengough and Stuart, B.P. 223999, 223995, 1923.

Bergala and Goraki, J.Expt.Theor.Phys., U.S.S.R., 1934, 4, 527.

Bitter, Phys.Rev., 1932, 41, 507.

Bitter, Introduction to Ferro-magnetism, McGraw Hill, 1937.

Blandin, Comptes Rendus, 1949, 228, 1718.

Blum and Hogaboom, Principles of Electroplating and Electroformin McGraw Hill, 1930.

Blum and Rawdon, Trans.Electrochem.Soc., 1923, 44, 305.

Bozorth, Phys.Rev., 1925, 26, 390.

Brown, Rev.Mod.Phys., 1945, 17, 15.

Burden, Brattain and Shockley, J.Chem.Phys., 1946, 14, 714.

Cabrera and Mott, Report on Progress in Physics, 1949, 12, 163.

Clark, Fish and Weeg, Proc.Phys.Soc., 1936, 18, 723.

Cochrane, Proc.Phys.Soc., 1936, 48, 723.

Drabble, 1949, Ph.D.Thesis, University of London.

Elmore, Phys.Rev., 1937, 51, 982.

Elleman and Wilman, Proc.Phys.Soc., 1948, 61, 164.

Elleman and Wilman, Proc.Phys.Soc., 1949, A.62, 344.

Evans and Wilman, Proc.Phys.Soc., 1950, 63, 298.

Feitknecht and Lenel, Helv.Chim.Acta, 1944, 27, 775.

Finch and Quarrell, Proc.Roy.Soc., 1933, 141, 398.

Finch and Quarrell, Proc.Phys.Soc., 1934, 46, 148.

Finch and Sun, Trans.Farad.Soc., 1936, 32, 852.

Finch and Williams, Trans.Farad.Soc., 1937, 33, 564.

Finch and Wilman, Ergeb.exakt.Naturwiss, 1937, 16, 353.

Finch, Wilman and Yang, ~~Trans~~.Farad.Soc.Disc., 1947, 43A, 144.

Finch and Whitmore, Trans.Farad.Soc., 1938, 34, 680.

Finch, Guthrie Lecture, 1950.

Finch, J.Chem.Soc, 1938.

Frisby, Comptes Rendus, 1949, 223, 1291.

Graham, Trans.Electrochem.Soc., 1923, 44, 427.

Halfawy, Ph.D.Thesis, University of London, 1948.

Harrington and Nelson, Amer.Inst.Min.Met. Tech.Bull., 1158.

Hedges, Protective Films on Metals, Chapman and Hall, 1932.

Hickling and Taylor, Trans.Farad.Soc., 1948, 44, 262.

Home and Maquestau, Journee des Etats de Surface. 1945, Oct.90.

Hothersall, Trans.Farad.Soc., 1935, 31, 1242.

Huber and Bieri, Helv.Chim.Acta., 1948, 21, 375.

Hume-Rothery and Wyllie, Proc.Roy.Soc., 1943, 181, 331.

Huntington, Trans.Farad.Soc., 1905, 1, 324.

Jacquet, Bull.soc.Chim.Franc., 1936, 3, 705.

Jenny, Anodic Oxidation of Aluminium and its Alloys, Griffin, 1940.

Kohlschutter and Schodl, Helv.Chim.Acta., 1922, 5, 593.

Lamchen, Ph.D.Thesis, University of London, 1937.

Mehl, McCandless and Rhines, Nature, 1934, 134, 1009.

Miyake, Sci.Pap.I.P.C.R., Tokyo, 1936, 26, 167.

Miyake, Sci.Pap.I.P.C.R., Tokyo, 1937, 31, 161.

Miyake, Sci.Pap.I.P.C.R., Tokyo, 1938, 34, 565.

Mott, Trans.Farad.Soc., 1947, 43, 429.

Muller, Trans.Farad.Soc., 1931, 27, 737.

Murison, Phil.Mag., 1934, 17, 96.

Nelson, J.Chem.Phys., 1937, 5, 252.

Neel, J.de Phys., 1944, 5, 241.

Palache, Berman and Frondel, Dana's System of Mineralogy, 1944

Preston and Bircumshaw, Phil.Mag., 1935, 20, 706.

Preston and Bircumshaw, Phil.Mag., 1936, 22, 654.

Royer, Bull.soc.Min.Franc., 1928, 51, 7.

Rudiger, Ann.Phys., 1937, 30, 505.

Schmidt, Zeit.Electrochem., 1908, 15, 53.

Siefert, Zeits.Krist., 1940, 102, 183.

Sun, Ph.D.Thesis, University of London, 1934.

Thomson, Proc.Roy.Soc., 1931, 133, 1.

Thomson, Proc.Phys.Soc., 1948, 61, 403.

Thomson and Cochrane, Theory and Practice of Electron Diffraction Macmillan, 1939.

Thirsk, Ph.D.Thesis, University of London, 1939.

Tunell, Posnjak and Ksanda, Zeit.Krist., 1935, 90, 120.

Tsuboi, Kyoto Coll.Sci.Mem., 1928, 11. 271

Tsuboi, Kyoto Coll.Sci.Mem., 1929, 12, 209.

Usmani, ~~Proc.Phys.Soc.~~ Phil. Mag., 1941, 32, 89.
I.H.

Van der Merwe, Disc.Farad.Soc., 1949, p.201.

Williams, Bozorth and Schockley, Phys.Rev. 1949, 75, 155.

Wilman, Proc.Phys.Soc., 1948, 52, 323.

~~Wilman, Proc.Phys.Soc., 1948, 52, 323.~~

Wilman, Nature, 1950, 165, 321.

Wood, Proc.Phys.Soc., 1931, 43, 138.

Wyckoff, Crystal Structure, 1948 (Interscience Pub.)

Yang, Ph.D.Thesis, University of London, 1948.

Yamaguti, Proc.Phys-Math.Soc.Japan, 1935, 17, 443.

Yamaguti, Proc.Phys-Math.Soc.Japan, 1938, 20, 230.